INFINITELY CONDUCTING DYNAMOS AND OTHER HORRIBLE EIGENPROBLEMS

By

B.J. Bayly

IMA Preprint Series # 886

October 1991

INFINITELY CONDUCTING DYNAMOS AND OTHER HORRIBLE EIGENPROBLEMS

B. J. BAYLY†

Abstract. The kinematic dynamo problem in the limit of infinite fluid conductivity leads to an eigenvalue problem of the form

$$\lambda \mathbf{f}(T(\mathbf{x})) = A(\mathbf{x})\mathbf{f}(\mathbf{x})$$

where T is a nonlinear transformation on a compact region and A is a matrix-valued function of position. Numerical simulations indicate that the "eigenfunctions" are singular or zero over almost the entire domain, but estimates of the eigenvalues are extremely accurate with quite modest resolution. Eigenproblems of this type also occur in the spectral theory of Schrödinger operators, hydrodynamic stability theory, and the thermodynamic formalism for dynamical systems theory.

Key words. dynamos, chaos, dynamical systems, magnetohydrodynamics, eigenvalue computations

§1. INTRODUCTION

The Earth's magnetic field is believed to be maintained by fluid flows and electric currents interacting in the fluid core. Prof. Roberts has just given a superb account of geodynamo modelling, emphasizing the interplay between convection, rotation, and electromagnetic (Lorentz) forces. Many of the same considerations also apply to solar and stellar dynamo modelling. The study of magnetic field maintenance in large bodies is vast, and the general references [1-5] listed in the bibliography are just a sample of the material available in book form, to say nothing of the literature in archival journals. My lecture will discuss a mathematical problem which is probably irrelevant for modellers, but which lies at the conceptual foundations of the whole subject.

Generally speaking, a dynamo is a flow of electrically conducting fluid capable of maintaining a magnetic field. Without external sources, any distribution of electrical current in a stationary body of conducting material will die away. If the material moves, however, new currents can be generated as the material crosses the magnetic field associated with the original current distribution. If the motion is strong enough, and if the new current reinforces rather than opposes the old current, this regeneration process can compensate for the inevitable losses due to Ohmic heating.

The name 'dynamo' comes from the dynamos, or generators, in that turn mechanical energy into electric power. Generators typically consist of a rotor on which are mounted coils of wire that spin in a stationary (stator) magnetic field. In a bicycle lamp generator the field comes from a permanent magnet. In a large power generator, supplying electricity to a city, the field is supplied by electromagnets, the

†Mathematics Department, University of Arizona, Tucson AZ 85721, USA. This work was supported by AFOSR Contract F9620-86-C0130 (with the U.R.I. program at the University of Arizona), and N.S.F. Grants EAR8902759 and DMS9057124

current that powers the electromagnets being part of the generator's output. Thus the field is required in order to produce current, but the field cannot exist without the current. It is not clear why any current is produced at all.

Although the state of zero current and zero magnetic field is a perfectly good equilibrium for a commercial generator, it is not necessarily stable. If the rotor is spinning at full speed, and a small magnetic fluctuation is introduced, the motion of the rotor will generate a small current fluctuation, which will flow through the stator coils and produce another magnetic field fluctuation, and so on. If the generator is built properly, and if the rotor is spinning fast enough, each new magnetic fluctuation will be stronger than the last, and the field will grow exponentially. The growth rate is determined by the design of the generator, the resistance of the wires, and the speed at which the rotor spins. Eventually the current will be so strong that the electromagnetic Lorentz force reacts back on whatever engine is powering the generator, and the field will saturate at the point where the electromagnetic torque equals the driving torque.

The same general scenario is believed to apply to conducting planetary and stellar interiors. It is perfectly possible for electrically conducting fluid to flow with no magnetic fields or currents present. This state could be similarly unstable to the simultaneous growth of magnetic fields and currents. If the magnetic field is weak, the Lorentz forces do not affect the fluid motion. The magnetic field then satisfies a linear evolution equation, and (presumably) grows exponentially at a rate determined by the properties of the fluid and its velocity field. When the field becomes strong, the Lorentz forces affect the fluid motion, and the system requires fully nonlinear magnetohydrodynamics for its description.

The right kind of material motion can sustain or amplify a distribution of electric currents and magnetic fields. The necessary energy comes from the particles doing mechanical work as they move through the Lorentz force field, and this mechanical energy must be supplied by some external agency. A power generator is driven by turbines that in turn are driven by burning fuel or running water. In the Earth, the core is stirred by compositional convection [6] . The Sun's dynamo is stirred by ordinary thermal convection whose energy source is nuclear reactions in the deep center [7] .

The linear equation describing magnetic field evolution in a material whose motion is known may have exponentially growing solutions, depending on the motion and the physical properties of the material. Using the generator analogy again, we obviously need to use a highly-conducting material for the wires, and we need to spin it above some critical speed before it the feedback process can beat the losses. Furthermore, the coils of the stator and rotor coils must be wound in the correct senses and appropriately placed to ensure that the feedback process is indeed positive rather than negative. Determining what kinds of motion and material properties result in positive feedback and exponentially growing solutions is the kinematic dynamo problem.

In the early days of dynamo theory, it was unclear whether kinematic dynamos with positive growth rates even existed. After all, a power generator requires in-

sulation to prevent current from flowing where it is not wanted, and the resulting current path has nontrivial topology. Whether the same type of feedback process could ever work in a simply connected body of fluid is not obvious. Indeed, some of the earliest work [8,9] consisted of proofs that kinematic dynamo action is impossible in two-dimensional or axisymmetric situations. The kinematic dynamo problem was not solved until Herzenberg [10] and Backus [11] produced explicit examples of flows in which magnetic fields would increase exponentially. These examples are artificial, but they serve the purpose of showing that the antidynamo theorems can be circumvented.

Steenbeck, Krause, and Radler [12] brought kinematic dynamo theory into the real world with their observation that any turbulent flow lacking statistical reflection invariance is a potential kinematic dynamo. Their so-called α-effect is a generic mechanism that can be expected to act in any large object with a turbulent conducting fluid interior. It is such a successful mechanism that many, perhaps even most, dynamo theorists feel that the kinematic dynamo problem is no longer a problem. The next step, which is still the center of dynamo research, is to incorporate the α-effect into detailed models of the solar and terrestrial interiors [13] . This research includes investigations of strong-field dynamos, in which the Lorentz forces are important ingredients of the dynamics.

Tucked away in all the mathematical treatment of these various dynamos is an assumption that the resistivity of the material is a fairly large number, or more precisely that the magnetic Reynolds number is small. The magnetic Reynolds number R_m is a dimensionless quantity, defined to be the product of a characteristic lengthscale of the flow and a characteristic velocity scale, divided by the magnetic diffusivity. This is because the larger R_m is, the more complicated is the small-scale structure of the magnetic field and current distributions. Disconcertingly, many of the examples that can be analyzed have the property that the dynamo efficiency goes to zero as $R_m \to \infty$ [14-16] . Since R_m is fairly high in the Earth's core and very high in the Sun's convection zone, it is important to discover whether we have just been doing the wrong examples, or whether some fundamental obstacle exists to dynamo action in very highly conducting fluids.

The fast dynamo problem is to elucidate the amplification process of magnetic fields in fluids of arbitrarily high conductivity [17] . Geophysicists, astrophysicists, and mathematicians have worked on the fast dynamo problem. Some have analyzed simple models [18-21] , some have numerically simulated more complex models [22-26] . Soward [27] produced a beautiful example of a simple flow, albeit containing weak singularities, that acts as a fast dynamo. Others have derived general sufficient conditions for the existence of fast dynamos [28,29] . Unfortunately, flows satisfying these conditions are necessarily topologically nontrivial [30] and may not even exist [31].

Since forward progress on the fast dynamo problem is difficult, lateral progress is an attractive alternative. That is, we can think about other problems from other branches of mathematics which have similar features. If we can solve any of these other problems - better still, if someone else has already solved them - we may get

useful information about the fast dynamo problem. At present, studying these other problems has served only to highlight the special features of the dynamo problem that make it hard. Nonetheless, these problems are still interesting models, full of nontrivial mathematics.

The problems I shall discuss can be thought of as coupled systems of advection-reaction-diffusion equations with linear chemistry. The quantities of interest are carried around by a given flow, possibly diffusing at the same time. In addition, each quantity is increasing or decreasing at a rate which is a linear combination of all the quantities. This structure is broad enough to include applications from hydrodynamic stability, reacting and diffusing systems, and dynamical systems theory in addition to dynamo theory. If the reader knows another problem that fits into the same pattern, the author would be most interested in learning about it.

§2. Dynamo theory

2.1. Background. Let us imagine a body of fluid in motion. In physical reality, we have in mind the interior of the Earth or the Sun, or perhaps a container of fluid in a laboratory. Mathematically, we think of the interior of a sphere or cube or some other compact object with a nice boundary. We denote by D the region occupied by fluid, and assume for simplicity that D does not change with time. We let $\mathbf{u}(\mathbf{x},t)$ denote the fluid velocity vector at the point $\mathbf{x}$ at time t. We assume that the flow is incompressible, so $\nabla \cdot \mathbf{u} = 0$ everywhere inside D. The boundary of the flow domain D is assumed impermeable to fluid, so $\mathbf{n} \cdot \mathbf{u} = 0$ everywhere on ∂D. In some mathematical idealizations, such as when D is a torus, D has no boundary and boundary conditions are immaterial.

If the fluid is a classical electrical conductor, the electromagnetic equations can be manipulated [1] to yield a single equation, the induction equation, for the magnetic field $\mathbf{B}(\mathbf{x},t)$. Using a characteristic length of D to measure lengths and a characteristic flow speed to measure velocities, the induction equation can be written in dimensionless form:

$$(\partial_t + \mathbf{u}\cdot\nabla)\mathbf{B} = [\nabla\mathbf{u}]\mathbf{B} + \varepsilon\nabla^2\mathbf{B}. \tag{2.1.1}$$

In (2.1.1), $[\nabla\mathbf{u}]$ is the velocity gradient tensor whose ij entry is $\partial u_i/\partial x_j$. The quantity ε is the dimensionless magnetic diffusivity, equal to the inverse of the magnetic Reynolds number.

The partial differential equation (2.1.1) is linear, with space-time dependent coefficients. We can rewrite it as

$$\partial_t \mathbf{B} = \mathcal{L}_\varepsilon \mathbf{B}$$

if we define the linear operator

$$\mathcal{L}_\varepsilon \mathbf{B} \equiv [\nabla\mathbf{u}]\mathbf{B} - \mathbf{u}\cdot\nabla\mathbf{B} + \varepsilon\nabla^2\mathbf{B}. \tag{2.1.2}$$

The appropriate boundary conditions for (2.1.1) are that $\mathbf{B}$ should match onto a potential field in the unbounded space around D (unless D has no boundary, of

course). With smooth initial data and a well-behaved velocity field, the subsequent evolution of the field is completely determined.

The magnetic field is assumed divergence-free in the derivation of (2.1.1); this is simply an article of faith on our part that magnetic monopoles do not exist. Dynamo theorists rarely worry about this condition, since the divergence of (2.1.1) yields

$$(\partial_t + \mathbf{u}\cdot\nabla)(\nabla\cdot\mathbf{B}) = \varepsilon\nabla^2(\nabla\cdot\mathbf{B})$$

which is the equation of motion for a passive scalar. Thus, if the initial condition for $\mathbf{B}$ is solenoidal, then $\nabla\cdot\mathbf{B}$ vanishes identically at all subsequent times. Also, if $\nabla\cdot\mathbf{B} \neq 0$ at time $t = 0$, then the divergent part of $\mathbf{B}(\mathbf{x},t)$ necessarily remains bounded in time. If we have any exponentially growing solution to (2.1.1), therefore, the divergence of the growing part must be divergence free.

The velocity field $\mathbf{u}(\mathbf{x},t)$ must be specified as part of the data for (2.1.1). It is natural to think about velocity fields with some kind of time-homogeneity. Examples are flows which are steady, periodic in time, quasiperiodic, or random in time with homogeneous statistics. With a time-homogeneous velocity field, we may expect solutions to eq. (2.1.1) that grow or decay exponentially. Since (2.1.1) is a functional evolution equation, we have to be careful with our definition of what constitutes exponential growth, but it seems safe to define the maximal growth-rate

$$\sigma_{\mathbf{u},\varepsilon} = \sup_{\mathbf{B}(\cdot,t=0)} \left[\lim_{t\to\infty} \frac{1}{t} \log \|\mathbf{B}(\cdot,t)\| \right]. \tag{2.1.3}$$

In (2.1.3) $\|\mathbf{B}(\cdot,t)\|$ denotes some functional norm of the magnetic field at the moment t. Armed with (2.1.3), we say that the flow $\mathbf{u}(\mathbf{x},t)$ is a dynamo with diffusivity ε if $\sigma_{\mathbf{u},\varepsilon} > 0$.

The definition of the growth rate obviously depends on the choice of norm and the space of allowed initial conditions. However, if $\varepsilon > 0$, $\mathcal{L}_\varepsilon$ will have a discrete spectrum of eigenvalues accumulating only at $-\infty$. The maximal growth rate $\sigma_{\mathbf{u},\varepsilon}$ will then be the real part of the eigenvalue(s) with largest real part. Thus, the question of whether $\mathbf{u}$ is a dynamo when the diffusivity equals ε can be answered by solving the eigenvalue problem

$$\mathcal{L}_\varepsilon \hat{\mathbf{B}}(\mathbf{x}) = \lambda \hat{\mathbf{B}}(\mathbf{x}) \tag{2.1.4}$$

and seeing whether any of the eigenvalues have positive real part. This is not difficult in practice, as standard numerical techniques [32,33] exist for finding the eigenvalues with largest real part of large matrices.

2.2. The fast dynamo problem. The growth-rate $\sigma_{\mathbf{u},\varepsilon}$ can be bounded above independently of the diffusivity. For example,

$$\sup_D \sum_{i,j=1}^{3} (\partial u_i/\partial x_j)^2$$

provides a coarse but easy upper bound. Therefore we can define

$$\sigma_{\mathbf{u},0+} \equiv \limsup_{\varepsilon \to 0+} \sigma_{\mathbf{u},\varepsilon}. \tag{2.2.1}$$

The flow $\mathbf{u}(\mathbf{x},t)$ is called a fast dynamo if $\sigma_{\mathbf{u},0+} > 0$. The fast dynamo problem is to characterize those flows, if they exist at all, which are fast dynamos.

If the flow $\mathbf{u}(\mathbf{x},t)$ is a fast dynamo, this means that the given fluid motion can amplify a magnetic field, no matter good an electric conductor the fluid is. This seems a strange thing to worry about. Our intuition, not to mention the experience of electrical engineers building power stations, suggests that if the positive feedback between field and current works at all with a poorly conducting material, it should work better in a highly conducting material. Remember, however, that an essential part of a power generator is the insulation between the wires; it would not work if the resistivity of the insulation went to zero.

The fast dynamo problem is hard because solutions of (2.1.1) can be complicated when ε is small. To see this, observe that except for the term $[\nabla \mathbf{u}]\mathbf{B}$, (2.1.1) is identical to three passive scalar advection-diffusion equations. With the stretching term $[\nabla \mathbf{u}]\mathbf{B}$ included, (2.1.1) has all the complexity of passive scalar dynamics, and more arises from the coupling of the different components.

If the diffusivity ε is set exactly to zero, (2.1.1) becomes the evolution equation for a field of differential line elements embedded in the fluid [34]. A differential line element can be thought of as a vector connecting two neighboring material particles. If the flow tends to separate the particles, the displacement vector lengthens. If the separation vector is initially parallel to the local magnetic field vector, these vectors will remain parallel, and the magnetic field will intensify exactly in proportion to the separation between the particles. This process is called magnetic field stretching. Efficient magnetic field amplification is therefore expected in flows which rapidly separate neighboring fluid particles. Vishik [29] showed that a necessary condition for fast dynamo action is that there exist at least one point whose neighbors recede from it exponentially fast.

Flows with the 'Lagrangian chaos' property separate neighboring fluid particles exponentially rapidly on s set of positive measure. Such flows are natural candidates for fast dynamos. Chaos is not sufficient for fast dynamo action, however. The problem is that even if the flow stretches magnetic field lines to many times their original lengths, the field lines must also get folded and twisted together so as to stay inside D. This folding process can easily bring fields pointing one direction into arbitrarily close proximity with fields pointing in other directions. In the presence of any finite diffusivity, these regions of opposite field merge and cancel, destroying much if not all of the field generated by stretching.

Total cancellation is guaranteed in two dimensions or three dimensional axisymmetric situations; this is the basis of the antidynamo theorems mentioned earlier. Cancellation can be avoided completely in some idealized examples, such as the rope dynamo [17] or the 'cat' dynamo [18], but at least some cancellation appears to be a feature of all realistic flows even in three dimensions. Unfortunately, it has

proved extremely difficult to quantify the concept of cancellation. A measure of cancellation would be of great help in understanding the dynamo problem.

2.3. Infinitely conducting dynamos. If ε is set to zero, (2.1.1) becomes

$$(\partial_t + \mathbf{u}\cdot\nabla)\mathbf{B} = [\nabla\mathbf{u}]\mathbf{B} \tag{2.3.1}$$

or

$$\partial_t \mathbf{B} = \mathcal{L}_0 \mathbf{B}$$

where $\mathcal{L}_0$ is just $\mathcal{L}_\varepsilon$ with $\varepsilon = 0$. Taking the divergence of (2.3.1) yields

$$(\partial_t + \mathbf{u}\cdot\nabla)(\nabla\cdot\mathbf{B}) = 0.$$

As before, if $\nabla\cdot\mathbf{B}$ vanishes identically at $t = 0$, then $\nabla\cdot\mathbf{B} \equiv 0$ for all $t > 0$. And even if $\nabla\cdot\mathbf{B} \neq 0$ initially, the divergence of any exponentially growing solution of (2.3.1) becomes negligible as $t \to \infty$ since the divergence is bounded by its initial amplitude.

It is tempting to study (2.3.1) by seeking eigenvalues and eigenfunctions satisfying

$$\mathcal{L}_0\hat{\mathbf{B}} = \lambda\mathbf{B}. \tag{2.3.2}$$

However, Moffatt and Proctor [35] showed that (2.3.2) can have no smooth eigenfunctions belonging to an eigenvalue with positive real part. Other approaches must be tried.

As stated in section II, (2.3.1) is identical to the equation for a field of material differential line elements in the fluid. The diffusive system (2.1.1) is a singular perturbation of (2.3.1), so it is possible that properties of the zero-diffusivity system do not imply anything about systems with small positive diffusivity or even the limit as the diffusivity goes to zero from above. However, if we ask the right questions about the diffusionless system, we stand an excellent chance of learning something useful about diffusive systems. In any case, it seems unlikely that the fast dynamo problem could be solved without any consideration of the perfectly conducting problem.

Since (2.3.1) is equivalent to a material equation, we need to be able to describe how material particles move in the flow. We define [36] $\mathbf{X}(\mathbf{a}, s|t)$ as the position at time t of the material particle that is at $\mathbf{a}$ at time s. $\mathbf{X}$ is a map taking the flow domain D to itself that represents the effect of the flow between the times t and s; $\mathbf{X}$ is therefore called the flow map. The chronological order of t and s is immaterial in defining the flow map. The flow map can be inverted simply by transposing t and s. Explicitly, if $\mathbf{x} = \mathbf{X}(\mathbf{a}, s|t)$, then $\mathbf{a} = \mathbf{X}(\mathbf{x}, t|s)$. The flow map satisfies the differential equation

$$\left(\frac{\partial}{\partial t}\right)_{s,\mathbf{a}} \mathbf{X}(\mathbf{a}, s|t) = \mathbf{u}(\mathbf{X}(\mathbf{a}, s|t), t). \tag{2.3.3}$$

Although written with partial derivatives, (2.3.3) is just a system of three coupled ordinary differential equations. Requiring

$$\mathbf{X}(\mathbf{a}, s|s) = \mathbf{a}$$

specifies a unique solution to (2.3.3).

The curves $\mathbf{X}(\mathbf{a}, s|t)$ with s and $\mathbf{a}$ fixed, $-\infty < t < \infty$ are the particle trajectories in the flow. They are also the characteristics of (2.3.1). Integrating (2.3.1) along characteristics yields the Cauchy formula [1]

$$\mathbf{B}(\mathbf{x}, t) = \mathbf{J}(\mathbf{X}(\mathbf{x}, t|s), s|t)\mathbf{B}(\mathbf{X}(\mathbf{x}, t|s), s). \tag{2.3.4}$$

Here $\mathbf{J}(\mathbf{a}, s|t)$ is the derivative matrix of $\mathbf{X}(\mathbf{a}, s|t)$:

$$\mathbf{J}_{ij}(\mathbf{a}, s|t) = \left(\frac{\partial}{\partial a_j} X_i(\mathbf{a}, s|t)\right)_{s,t}.$$

If the magnetic field is given everywhere at $t = 0$, the Cauchy formula determines the field at all future and past times; the absence of diffusion makes (2.3.1) time-reversible.

The rate of exponential growth of solutions to (2.3.1) can be quantified using (2.3.4). If $\|\cdot\|$ denotes a matrix norm, we define the (first) Lyapunov [37] exponent of the flow at the point $\mathbf{a}$ by

$$\lambda_{\mathbf{u}}(\mathbf{a}, s) = \lim_{t\to\infty} \log \|\mathbf{J}(\mathbf{a}, s|t)\|.$$

Positivity of $\lambda_{\mathbf{u}}(\mathbf{a}, s)$ means that a magnetic field vector moving with the fluid particle that goes through $\mathbf{a}$ at time s is almost sure to stretch exponentially forever. If the flow has Lagrangian chaos with positive Lyapunov exponent on a set of positive measure, we expect to see plenty of efficient magnetic field amplification. Since the diffusivity is zero, regions of fluid with equal and oppositely directed magnetic fields may be brought together arbitrarily closely by the mixing action of the flow.

An observer measuring the magnetic field with an instrument of finite resolving power might not be able to see the small scale structure. If the test section of the magnetometer were much larger than the scale on which regions of different field are mixed, it would indicate a field of much smaller strength than the true magnitude of the field. Even if the field strengths at individual points are increasing exponentially, the field averaged over a small fixed volume in space might remain bounded in time or decay. The arbitrarily intimate mixing of fluid containing differently directed magnetic fields is the diffusionless analogue of the cancellation phenomenon discussed in the last section. We would like a definition of dynamo action at zero diffusivity that allows for cancellation.

The measurement process for a real magnetometer is best described by saying that the magnetometer has some characteristic aperture function which is large in

the test section and which goes to zero smoothly with distance from the test section. The output is the integral over the flow domain of the magnetic field multiplied by the aperture function. We say that the flow $\mathbf{u}(\mathbf{x},t)$ is an *infinitely conducting dynamo* if there exists a smooth vector function $\mathbf{g}(\mathbf{x})$ and a smooth initial condition $\mathbf{B}(\mathbf{x},t=0)$ for (2.3.1), for which

$$\sigma_{\mathbf{u},0} \equiv \lim_{t\to\infty} \frac{1}{t} \log\left| \int_D \mathbf{g}(\mathbf{x}) \cdot \mathbf{B}(\mathbf{x},t) d\mathbf{x} \right| > 0. \tag{2.3.5}$$

Note that the definition of an infinitely conducting dynamo is different from the definition of a fast dynamo. The limiting value in (2.3.5) might equal $\sigma_{\mathbf{u},0+}$ defined in the previous section, for 'generic' functions g and $\mathbf{B}(\mathbf{x},t=0)$, or it might not; no results of this nature are known. It is known, by the way, that neither dynamo growth rate is necessarily related to the Lyapunov exponents [25,28]. We believe that flows which are infinitely conducting dynamos are also fast dynamos, and vice versa, but we lack definite information about the correspondence.

Formula (2.3.5) embodies an idea which is relatively new in dynamo theory, although obvious in retrospect. At finite ε, the dynamo problem is solved by finding eigenfunctions of the diffusive operator $\mathcal{L}_\varepsilon$. The Moffatt-Proctor results, however, indicate that the eigenfunction approach is useless for the infinitely conducting dynamo problem, at least if we are expecting a function as the answer. But (2.3.5) says it does not matter if the magnetic field is not an ordinary function; all we need is that $\mathbf{B}$ multiplied by any smooth function be a measurable function [38]. Finn and Ott [20,25] use a very similar idea, measuring dynamo action by integrating the flux of $\mathbf{B}$ across a fixed surface in space.

Thus we can use the eigenproblem approach if we allow 'eigenfunctions' in the space of distributions on D. This is equivalent to seeking the residual spectrum of the operator $\mathcal{L}_0$. We recall that the usual eigenvalue problem, in which eigenfunctions are sought in the form of ordinary smooth functions on D, delivers only elements of the point spectrum.

Saying that $\mathbf{B}(\mathbf{x},t)$ is a distribution means that for any smooth function of position $\mathbf{g}(\mathbf{x})$, we can define a number

$$\langle \mathbf{g}, \mathbf{B} \rangle = \int_D \mathbf{g}(\mathbf{x}) \cdot \mathbf{B}(\mathbf{x},t) d\mathbf{x},$$

and that the map taking $\mathbf{g}$ to $\langle \mathbf{g}, \mathbf{B} \rangle$ is a linear transformation. Any ordinary function is a distribution, but not all distributions are functions.

Since distributions are not necessarily differentiable, we cannot determine whether a distribution $\mathbf{B}$ is a solution of (2.3.1) by plugging it in. However, if $\mathbf{B}$ were differentiable in both space and time and satisfied (2.3.1), we could take the dot product of (2.3.1) with any smooth function $\mathbf{h}(\mathbf{x},t)$ and integrate. Since we are interested in the differential equation rather than the boundary conditions, we restrict attention to functions $\mathbf{h}$ whose support never intersects the boundary, and call such functions test functions.

Integration by parts allows all derivatives to be thrown onto $\mathbf{h}$, and the boundary terms vanish since $\mathbf{h}$ and all its derivatives are zero at the boundary. Thus

$$\frac{d}{dt}\int_D \mathbf{h}(\mathbf{x},t)\cdot\mathbf{B}(\mathbf{x},t)d\mathbf{x} = \int_D \left((\partial_t + \mathbf{u}\cdot\nabla)\mathbf{h} + [\nabla\mathbf{u}]^T\mathbf{h}\right)\cdot\mathbf{B}(\mathbf{x},t)d\mathbf{x} \tag{2.3.6}$$

for any test function $\mathbf{h}$. Now (2.3.6) does not depend on differentiability of $\mathbf{B}$ in either space or time, so it makes sense even if we plug in a distribution. So we say that $\mathbf{B}(\mathbf{x},t)$ is a solution of the zero-diffusivity induction equation (2.3.1) in the distributional sense if (2.3.6) is satisfied for any smooth function $\mathbf{h}(\mathbf{x},t)$ whose support never intersects ∂D.

Any distributional solution of (2.3.1) should also satisfy the appropriate form of the solenoidality condition. For ordinary functions, $\nabla\cdot\mathbf{B}=0$ implies that

$$\int_D \mathbf{B}(\mathbf{x},t)\cdot\nabla\phi(\mathbf{x})d\mathbf{x} = 0 \tag{2.3.7}$$

for any smooth scalar function ϕ whose support does not intersect ∂D. Since (2.3.7) also makes sense for distributions, we say that $\mathbf{B}(\mathbf{x},t)$ satisfies the solenoidality condition in the distributional sense if (2.3.7) is satisfied for any scalar test function.

If we try a test function $\mathbf{h}(\mathbf{x},t)=\nabla\phi(\mathbf{x},t)$ in equation (2.3.6), we obtain

$$\frac{d}{dt}\int_D \mathbf{B}(\mathbf{x},t)\cdot\nabla\phi(\mathbf{x},t)d\mathbf{x} = \int_D \mathbf{B}(\mathbf{x},t)\cdot\nabla\left((\partial_t+\mathbf{u}\cdot\nabla)\phi(\mathbf{x},t)\right)d\mathbf{x}. \tag{2.3.8}$$

Thus, if the distribution $\mathbf{B}(\mathbf{x},t)$ is solenoidal in the distribution sense at $t=0$, and satisfies the distributional evolution equation (2.3.6), then $\mathbf{B}(\mathbf{x},t)$ is solenoidal at all other times. However, if $\mathbf{B}(\mathbf{x},t)$ is not solenoidal at $t=0$, (2.3.8) gives no bound on the rate at which the divergent part of $\mathbf{B}(\mathbf{x},t)$ increases in time. Violations of the solenoidality condition are not as harmless when dealing with distributions as they are when dealing with ordinary functions.

§3. Computations

One way to investigate the dynamo problem is to simulate the dynamo equation (2.1.1) numerically as an initial value problem, and observe whether the solutions grow exponentially. This is a straightforward problem, and excellent methods exist for solving such linear parabolic partial differential equations [39].

When the diffusivity is small, the domain D must be subdivided into a large number of very small cells in order to resolve the complex structure anticipated at small scales. Even if the diffusion is treated implicitly, the time step used in a high resolution computation must be of the same order of magnitude as, or smaller than, the size of a computational cell. Otherwise the method will be unstable due to violation of the CFL condition [40,41]. If we want to simulate the equations for times long enough to observe convincing exponential growth, the computational time could become prohibitively large.

An alternative strategy would be to simulate the Cauchy solution. The drawback is that the Cauchy solution requires knowledge of the particle trajectories,

which can only be found by solving the initial value problem (2.3.3). Furthermore, if the flow is chaotic, these solutions become extremely complicated at large values of t. If we use a flow for which the initial value problem can be solved easily for short finite times, however, we might be able to use the Cauchy formula advantageously. Since we are interested in the question of whether *any* flow can act as a fast dynamo, it is legitimate to start with flows whose main characteristic is that they are easy to compute with. This argument may be already familiar in its application to the gentleman who searches for his car keys only under the lampposts.

3.1. Pulsed flow models. A number of authors [18-20] have considered one dimensional models of fast dynamo action. These models are instructive and easy to simulate at very high resolution, but definitely artificial. Simulations of the induction equation (2.1.1) with an explicit velocity field require at least two dimensions.

We would also like the flows in our simulations to exhibit Lagrangian chaos, since this provides an effective mechanism for amplifying magnetic fields. But we also want flows for which we can easily compute the trajectories of fluid particles. These two requirements seem to be incompatible; one definition of Lagrangian chaos is that the particle trajectories not be integrable. A suitable compromise is to take two or more integrable flows in D and let them take turns acting on the fluid.

For example, we can let the velocity field be given by one explicitly integrable formula for $0 \le t < \tau/2$, by a different explicitly integrable formula for $\tau/2 \le t < \tau$, then by the first again for $\tau \le t \le 3\tau/2$, then by the second again, and so on. This alternating sequence of flows is likely to be at least partially chaotic unless there is some connection between the two integrable flows. At the same time, since each is explicitly integrable, the time-τ map can be expressed as the composition of the explicit integration formulas of the flows. Since the flow consists of pulses of one ingredient alternating with pulses of the other, we call this a pulsed flow model. The use of pulsed flow models in dynamo theory goes back to the original model of Backus [11].

Let T represent the displacement of fluid particles during the time interval $0 \le t < \tau$ in such a pulsed flow. The diffusionless magnetic field change over the same time interval can also be described in terms of T. If we write $\mathbf{J}(\mathbf{a})$ as an abbreviation for $\mathbf{J}(\mathbf{a}, 0|\tau)$ and $\mathbf{B}_n(\mathbf{x})$ for $\mathbf{B}(\mathbf{x}, n\tau)$, Cauchy's formula becomes

$$\mathbf{B}_{n+1}(\mathbf{x}) = \mathbf{J}(T^{-1}(\mathbf{x}))\mathbf{B}_n(T^{-1}(\mathbf{x})) = \{\mathcal{M}_0\mathbf{B}_n\}(\mathbf{x}). \tag{3.1.1}$$

Again, if $\mathbf{B}_0(\mathbf{x}) = \mathbf{B}(\mathbf{x}, t = 0)$ specified, then (3.1.1) determines the field configuration at all times which are integer multiples of τ.

The operator $\mathcal{M}_0$ is nicer than $\mathcal{L}_0$, even though both describe the same process. The main advantage of $\mathcal{M}_0$ is that it is a bounded operator while $\mathcal{L}_0$ is unbounded due to the presence of the $\mathbf{u} \cdot \nabla$ derivative. Also, $\mathcal{M}_0$ has similar structure to the unitary Koopman operator [42], which plays a major role in ergodic theory. Some properties of $\mathcal{M}_0$ in the context of Anosov diffeomorphisms were established by Mather [43] and recently applied to the dynamo problem by de la Llave [44].

In order to simulate (3.1.1) numerically, we need to discretize the space dependence of the magnetic field. The general procedure is to decide on some finite

set of basis functions suitable for representing the field, and to define a projection operator $\mathcal{P}$ that projects the infinite-dimensional space of possible magnetic fields down onto the subspace spanned by the chosen basis functions. The action of $\mathcal{M}_0$ on the infinite-dimensional space is then approximated by the finite-dimensional matrix $\mathbf{M}_0 = \mathcal{P}M_0\mathcal{P}$ acting on the finite-dimensional computational subspace. The numerical simulation of (3.1.1) then becomes nothing more than acting on the finite-dimensional field over and over with the matrix $\mathbf{M}_0$.

Once the simulation is programmed, we can run it with arbitrary initial condition and see whether the field grows exponentially. Typically the solution will settle down to a pattern in which successive iterates of (3.1.1) have the same spatial structure and the magnitude increases by a the same factor with every iteration. In this situation, the spatial structure is the eigenfunction of the $\mathbf{M}_0$ belonging to the eigenvalue with the largest absolute value, and the factor by which the magnitude increases with each iteration is the absolute value of that eigenvalue. Essentially, we are just finding the largest eigenvalue of $\mathbf{M}_0$ by the power method. Any numerical simulation along these lines is essentially specified by the nature of the pulsed flow, and by the finite-dimensional computational space.

3.2. Method. This section describes an implementation of the kind of numerical simulation described in the last subsection.

The domain D of the numerical simulations will be the square $0 \le x, y \le 2\pi$. Opposite edges are identified to give the square the topology of the 2-torus. That is, if a fluid particle flows across one edge of the square, it is immediately reintroduced at the corresponding point on the opposite edge of the square. Once the square becomes a torus it loses its boundary, so boundary conditions are unnecessary. Given an integer p, each edge of the square is divided into $N = 2^p$ identical little intervals of side $h = 2\pi/N$. The tensor product of these edge decompositions gives a decomposition of D into N^2 identical little square cells. The nodes of the grid, or grid points, are the corners of the squares. The coordinates of the (j, k) gridpoint are then (jh, kh), for $0 \le j, k \le N - 1$.

Next we need to define the projection $\mathcal{P}$. Suppose a function $f(x, y)$ is defined on the square. We define its discrete Fourier transform $\tilde{f}(l, m)$ by

$$\tilde{f}(l,m) = N^{-2} \sum_{j,k=-N/2}^{N/2-1} \exp\left[-2\pi i(lj + mk)/N\right] f(jh, kh)$$

for $-N/2 \le l, m \le N/2 - 1$. Then we define

$$[\mathcal{P}f](x,y) = \sum_{l,m=-N/8}^{N/8-1} \tilde{f}(l,m) \exp\left[i(lx + my)\right]. \tag{3.2.1}$$

It is simple to verify that $\mathcal{P}$ satisfies the defining property of projections, that $\mathcal{P}^2 = \mathcal{P}$. The reason for summing over such a restricted set of Fourier modes in (3.2.1) is partly to ensure that aliasing effects do not enter into the computation, and partly to make $\mathcal{P}f$ look like a smooth function on the lengthscale h.

The flows used in the simulations are pulsed Beltrami flows [45,46]. These are popular flows for dynamo computations [24,25,47], since they are simple to work with and display all kinds of interesting behavior. They are periodic in time with period $\tau = 1$, and are defined by

$$\mathbf{u}(\mathbf{x},t) = 2\alpha \begin{pmatrix} -\sin(y-\phi) \\ 0 \\ \cos(y-\phi) \end{pmatrix} \quad if \quad 0 \le t < 1/2 \tag{3.2.2}$$

and

$$\mathbf{u}(\mathbf{x},t) = 2\alpha \begin{pmatrix} 0 \\ \cos(x-\phi) \\ -\sin(x-\phi) \end{pmatrix} \quad if \quad 1/2 \le t < 1.$$

Here $\phi = (1+\sqrt{5})/2$ is an irrational phase shift introduced to move the stagnation points of the flow away from exact coincidence with grid points.

The motion of fluid particles can be easily computed for each phase of the motion. If $\mathbf{X}(\mathbf{a},0|t) = (X(t),Y(t),Z(t))$, then

$$X(1/2) = X(0) - \alpha\sin(Y(0)-\phi),$$

$$Y(1/2) = Y(0),$$

$$Z(1/2) = Z(0) + \alpha\cos(Y(0)-\phi),$$

followed by

$$X(1) = X(1/2),$$

$$Y(1) = Y(1/2) + \alpha\cos(X-\phi), \tag{3.2.3}$$

$$Z(1) = Z(1/2) - \alpha\sin(X-\phi).$$

The derivative matrix for the transformation T is

$$\mathbf{J}(\mathbf{a}) = \begin{pmatrix} 1 & 0 & 0 \\ -\alpha sin(X(1/2)-\phi) & 1 & 0 \\ -\alpha cos(X(1/2)-\phi) & 0 & 1 \end{pmatrix} \begin{pmatrix} 1 & -\alpha cos(Y(0)-\phi) & 0 \\ 0 & 1 & 0 \\ 0 & -\alpha sin(Y(0)-\phi) & 1 \end{pmatrix}. \tag{3.2.4}$$

As $\alpha \to 0$, the pulsed Beltrami flow (3.2.2) goes, in the sense of particle trajectories, to the steady flow

$$\mathbf{u}(\mathbf{x}) \sim \alpha \begin{pmatrix} -\sin(y) \\ \cos(x) \\ \cos(y) - \sin(x) \end{pmatrix}.$$

This flow is exactly integrable; all particles move on surfaces of constant $\psi(\mathbf{x}) = \cos(y) - \sin(x)$. Since $\psi(\mathbf{x})$ is actually the z-velocity component, this implies that all particles translate uniformly in z.

To check the ergodic properties of the pulsed Beltrami flows, we constructed Poincare sections. The Poincare section of a single fluid particle is taken to be its projected positions on the x, y plane at the times $t = 0, 1, 2, \cdots$, i.e. at the beginning of each new pulse of the flow. The pictures in figure 1 are actually superpositions of 144 individual Poincare sections, with each particle starting at one node of a uniformly spaced 12 by 12 grid in D. Figure 1a shows the Poincare sections when $\alpha = 1$. This value of α is a small number for the purposes of this system, and most of the trajectories lie on KAM tori. The tori begin to break up visibly when $\alpha = 2$, as shown in figure 1b. The tori are seriously disrupted at $\alpha = 3$ (figure 1c) and cannot even be detected (if they still exist) when $alpha = 5$ (figure 1d). Varying α between 0 and 5 allows us to tune the size of the region of Lagrangian chaos when we perform the numerical computations.

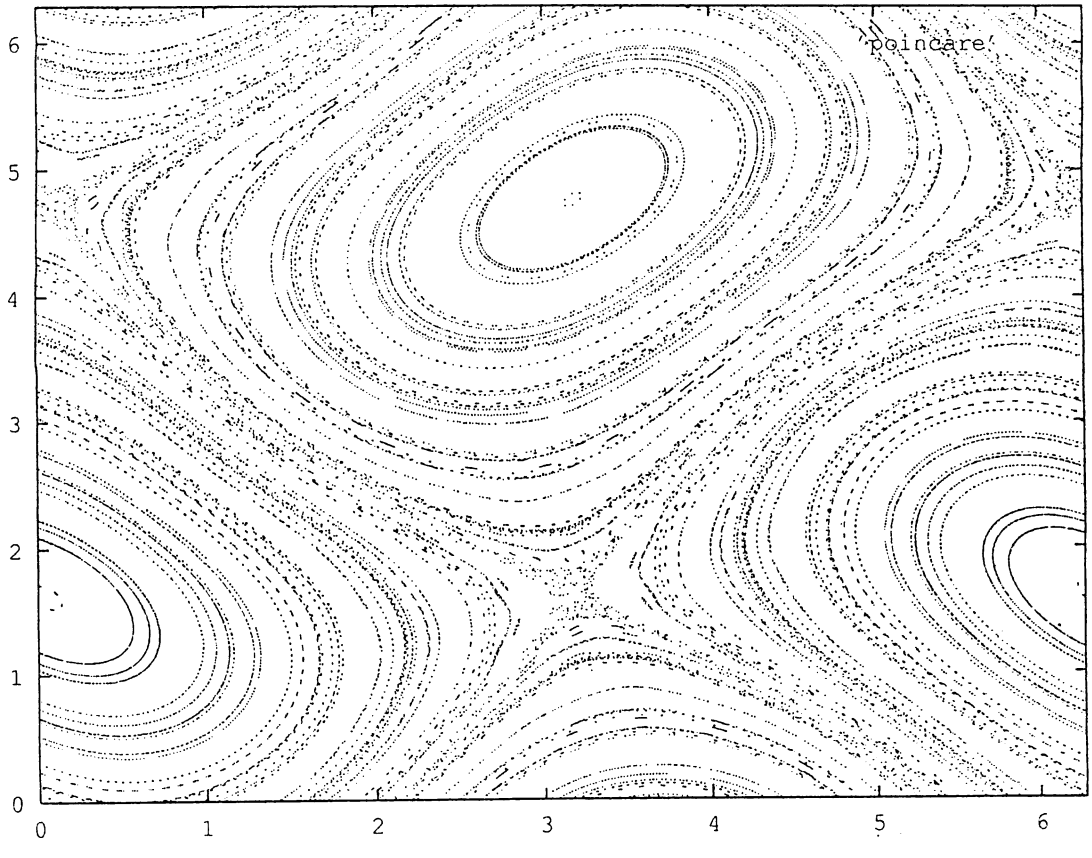

Figure 1a.

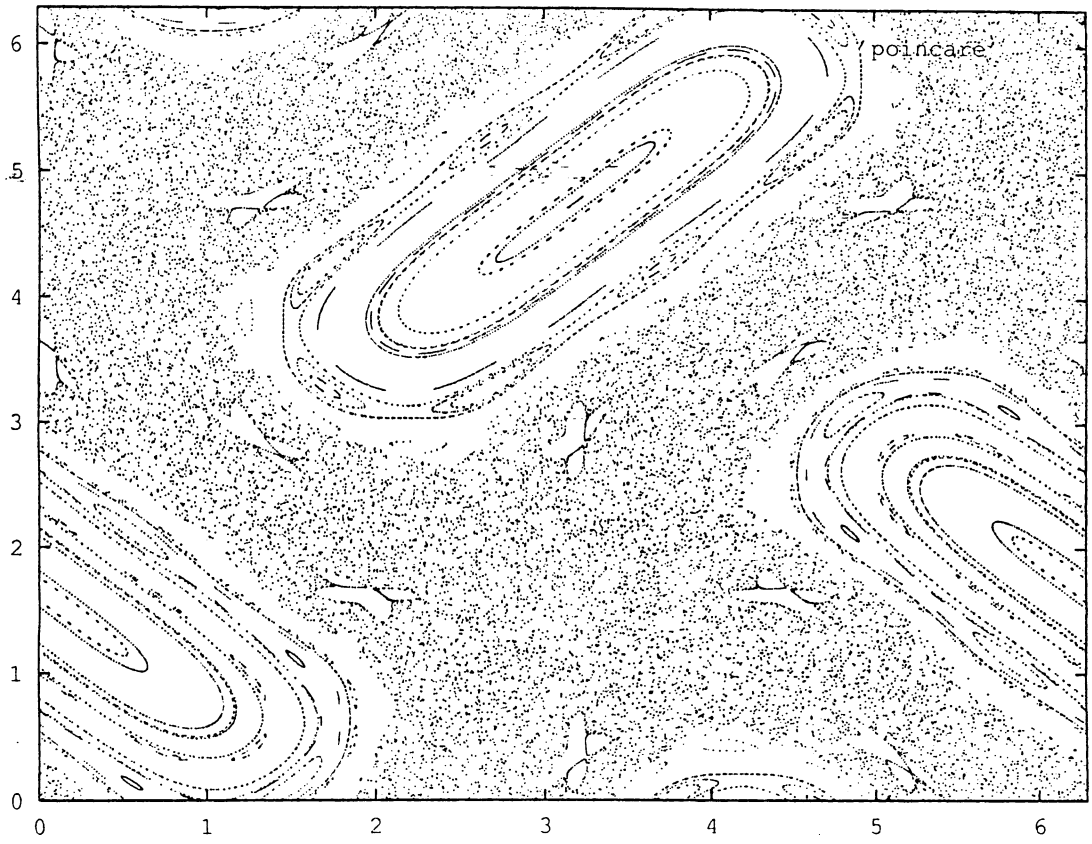

Figure 1b.

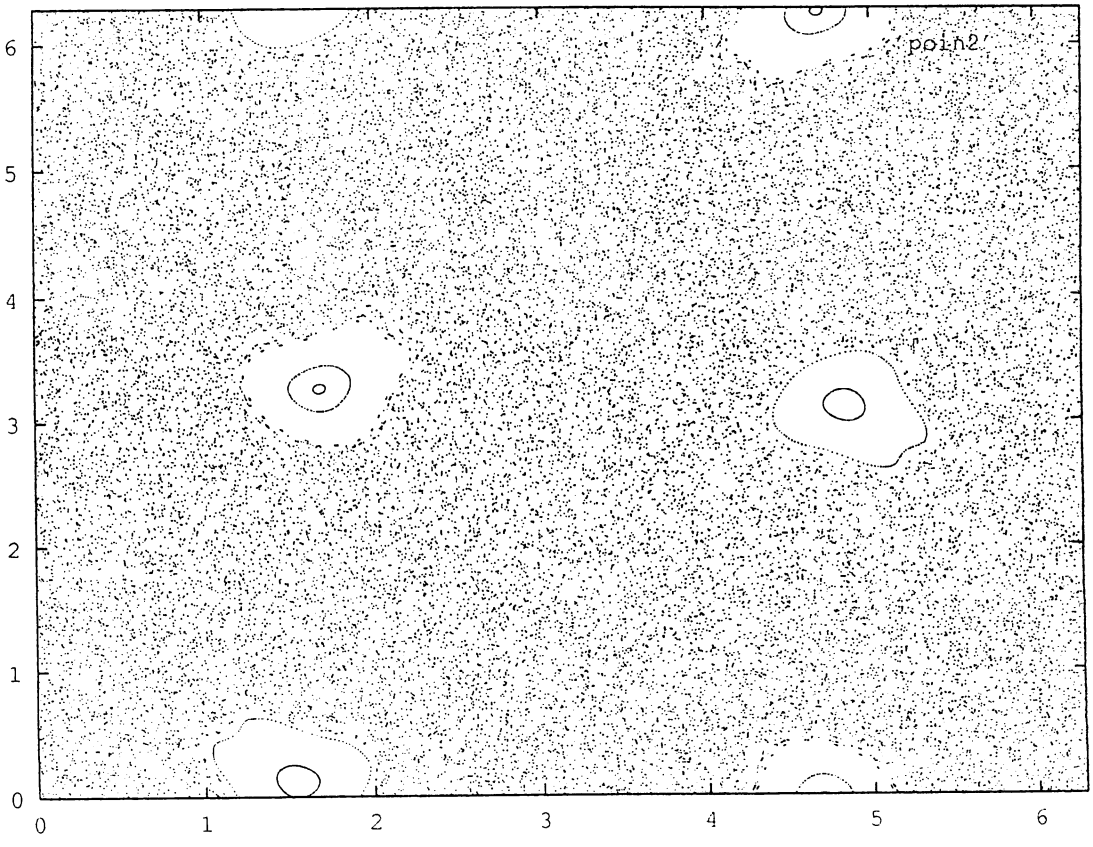

Figure 1c.

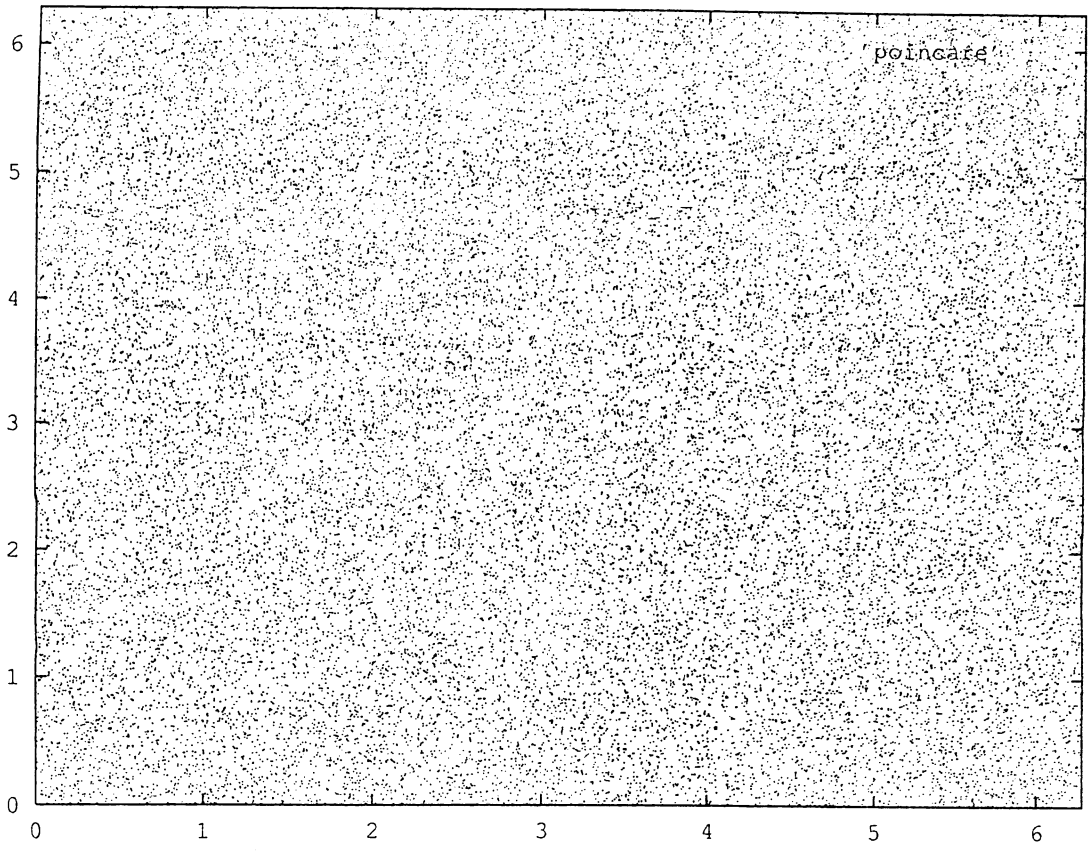

Figure 1d.

Figure 1. Poincaré sections for pulsed Beltrami flows. (a) $\alpha = 1$. (b) $\alpha = 2$. (c) $\alpha = 3$. (d) $\alpha = 5$.

The pulsed Beltrami flow (3.2.2) is quasi-two-dimensional; there are three nontrivial velocity components which depend on only two coordinates x, y. The third velocity component is required to make the problem three dimensional, for we know already that a purely two-dimensional dynamo cannot exist. However, the fact that the velocity field is independent of z allows the z-dependence of any magnetic field to be separated into Fourier modes of the form

$$\mathbf{B}_n(\mathbf{x}) = \bar{\mathbf{B}}_n(x, y) \exp(ikz) \tag{3.2.5}$$

which evolve completely independently. The evolution of any field of the form (3.2.5), assumed 2π periodic in x, y, can be simulated on the two-dimensional domain D. Restricting the nontrivial structure to the x, y plane allows us to get more spatial resolution for a given computational effort.

To simulate (3.1.1), we decide how many cells to divide the domain D into, and the flow parameter α and the wavenumber k. Then we take an arbitrary initial condition $\bar{\mathbf{B}}_0(x, y)$, and act on it repeatedly with the spatially discretized operator $\mathbf{M}_0$. Apart from the spatial discretization error, this results in completely faithful simulation of the diffusionless magnetic field evolution.

3.3. Results. If the discretized operator has one eigenvalue whose magnitude is greater than that of any other eigenvalue, the structure of the discretized magnetic

field will rapidly approach the eigenvector belonging to the dominant eigenvalue. The factor by which it grows at each iteration will be the magnitude of the dominant eigenvalue. In order to avoid overflow, the field is rescaled at every iteration, so the growth factor is actually the rescaling factor. In our computations, we iterate until this factor changes by less than 10^{-4} from one iteration to the next. The results of the computation are the approximate growth rate

$$\sigma_{numeric} = \log(rescaling\ factor)$$

and the field $\bar{\mathbf{B}}_n(x, y)$ returned at the end of the final iteration. This field is a good approximation to the dominant eigenfunction of the spatially discretized operator $\mathbf{M}_0$.

The first thing to be investigated in any numerical simulation is convergence as the resolution improves. As a typical test case, we set $\alpha = 3$, $k = 1.$, and ran the simulation for $N = 2^p$, with p ranging from 1 to 9. The computed growth rates are plotted in figure 2 against p for $p \geq 3$. The very coarsest simulations, with two and four cells in each direction, gave negative growth rates. Clear convergence is observed, with good agreement at $N = 32$ and variations of less than 1 per cent for $N \geq 128$.

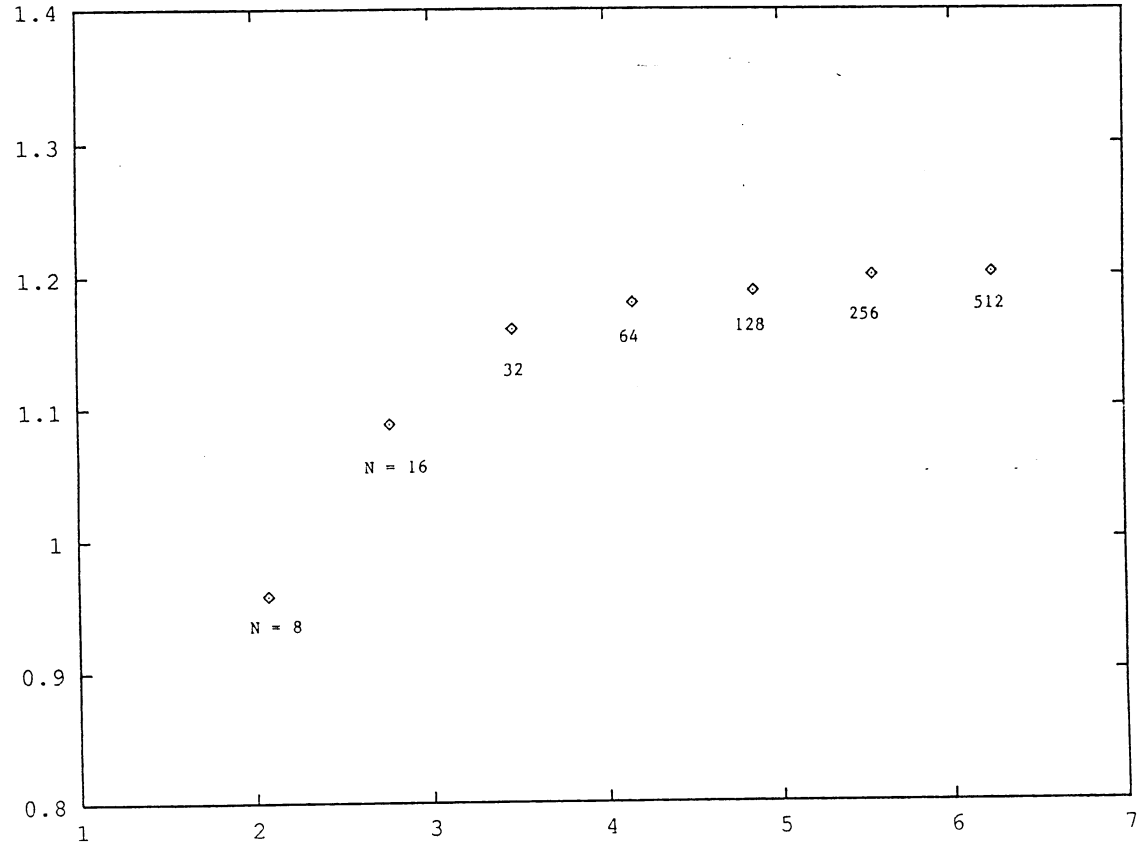

Figure 2. Convergence of computed dynamo growth rates with increasing resolution (see text for details). The vertical axis is the growth rate, while the horizontal axis is the natural logarithm of the number N of cells on each side of the square D. Each point is labelled with the corresponding value of N.

The computed eigenfunctions have very different structures at different resolutions, even at the same values of the other parameters. In figure 3 we plot the contours of $\log(\max(1, |\bar{\mathbf{B}}_n(\mathbf{x})|)$ in D at $N = 128$ and $N = 256$. There is much more complicated small-scale structure in the higher-resolution picture, despite the fact that the eigenvalues are almost the same. The reason we take the logarithm is that the eigenfunctions are so wild in their spatial dependence that plotting the contours of $|\bar{\mathbf{B}}_n|$ would convey almost no information.

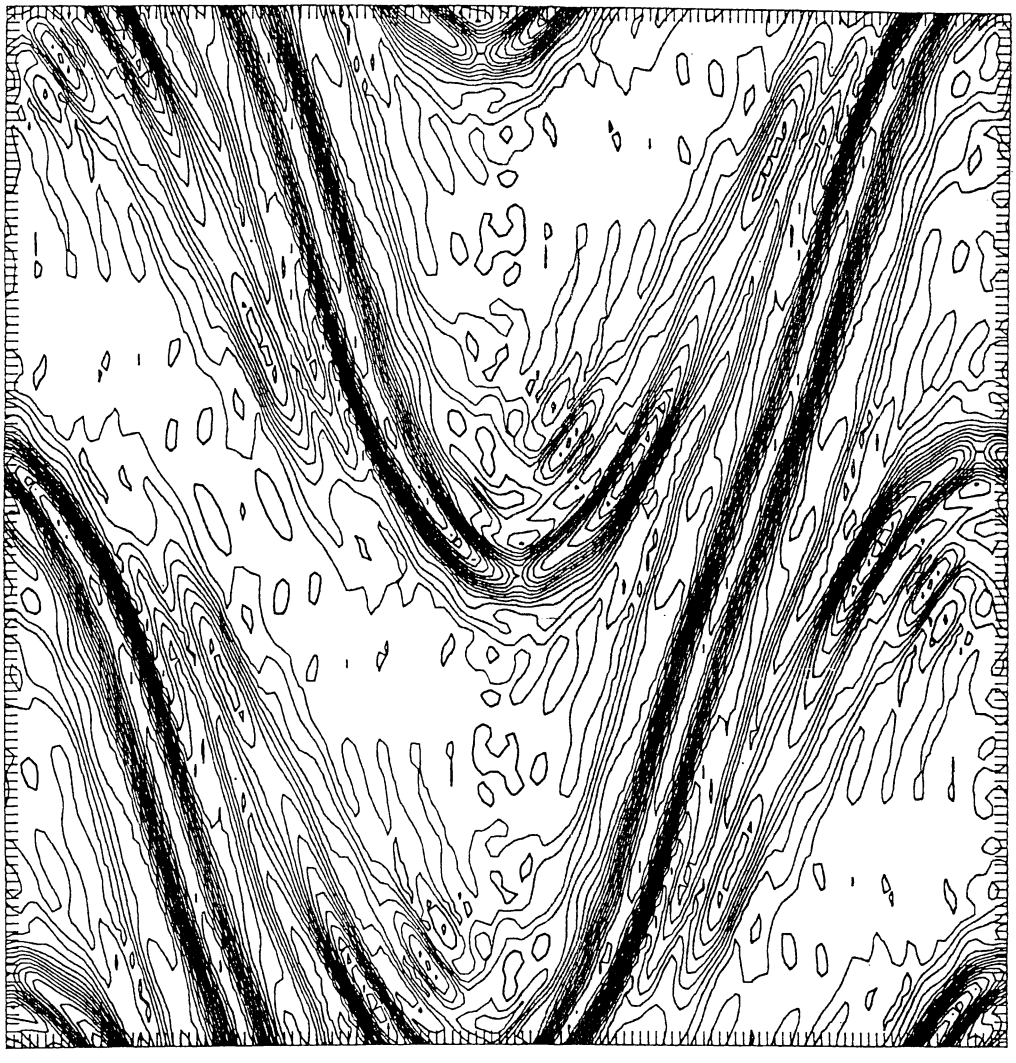

Figure 3a

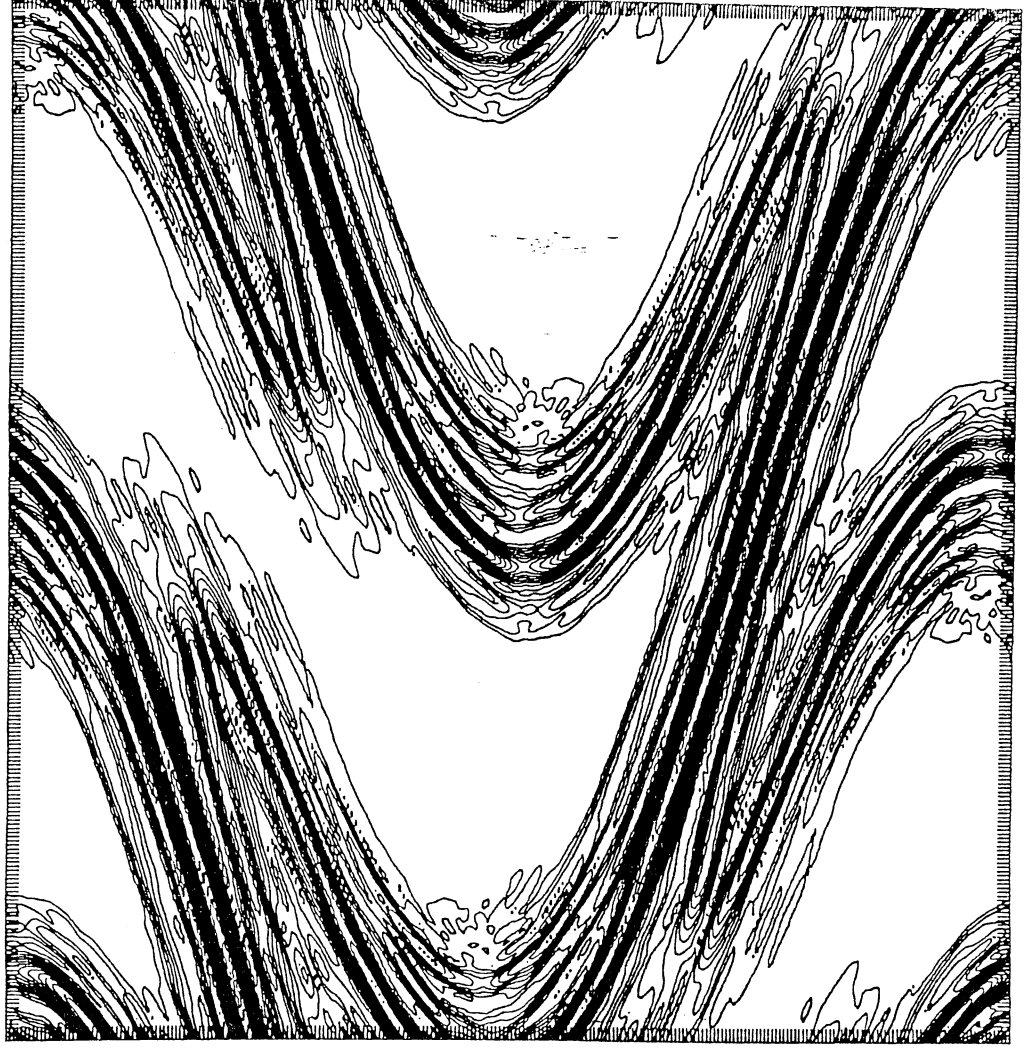

Figure 3b

Figure 3. Logarithmic contour plots of dominant dynamo eigenfunction at resolutions (a) $N = 128$ and (b) $N = 256$.

Next we simulated the magnetic field equations for various values of k at fixed $\alpha = 3$, at $N = 128$ resolution. Figure 4 shows the growth rate plotted as a function of k. One feature to notice is that the growth rate is zero at $k = 0$, which agrees with the antidynamo theorem prohibiting dynamo action in purely two-dimensional dynamics. For nonzero, but not very large, values of k robust growth occurs, with the peak growth rate occurring for k close to 1. At values of k larger than about 2, the jagged shape of the curve suggests that 128 cells in each direction may no longer be sufficient resolution to capture the essence of the dynamics.

We also computed the growth rate as a function of α with $k = 1$ fixed, at $N = 128$ resolution. Again there is a range of parameter values over which the dependence of the growth rate is reliably calculated, but for α greater than about 4 or so we lose confidence. This may reflect a tendency for more small scale magnetic field structure to be generated when each pulse of the flow lasts longer and shears the material more. For comparison with some results to be presented later, note that the growth rate is numerically considerably smaller than α at each value considered.

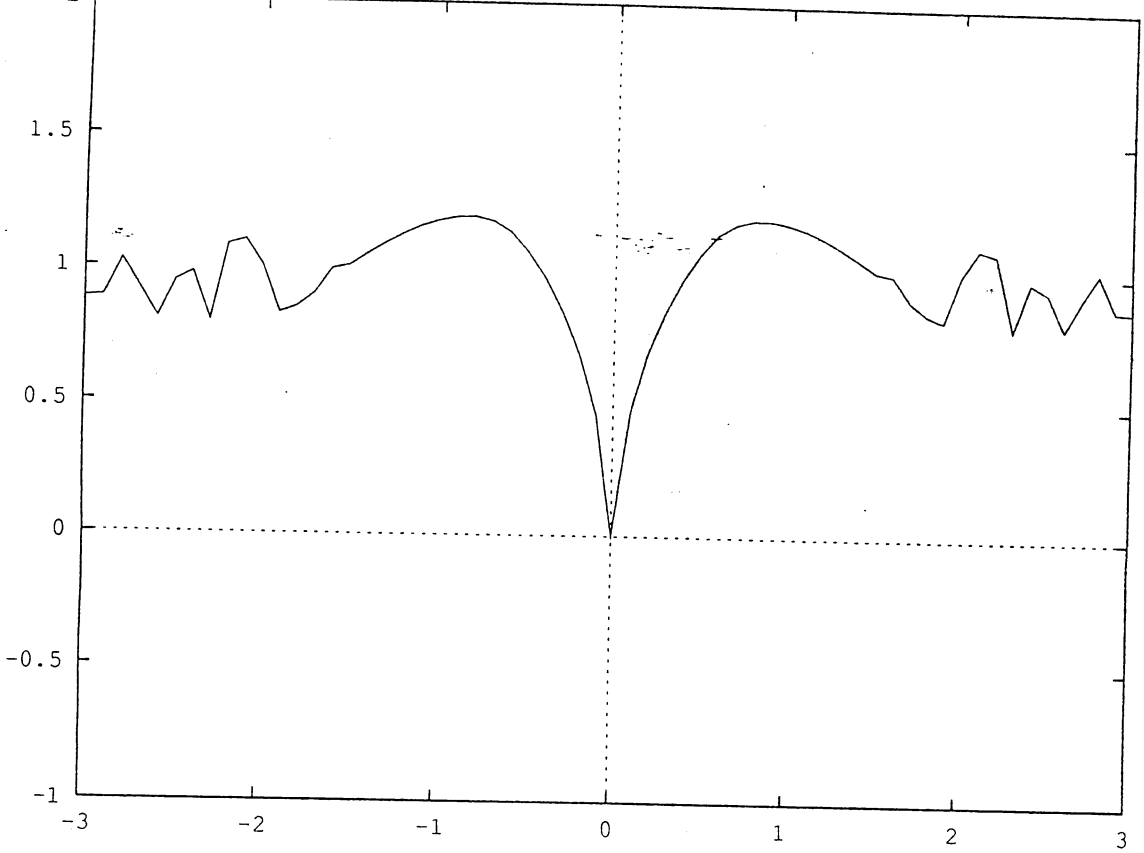

Figure 4: Dynamo growth rate as a function of z-wavenumber k, with other parameters fixed.

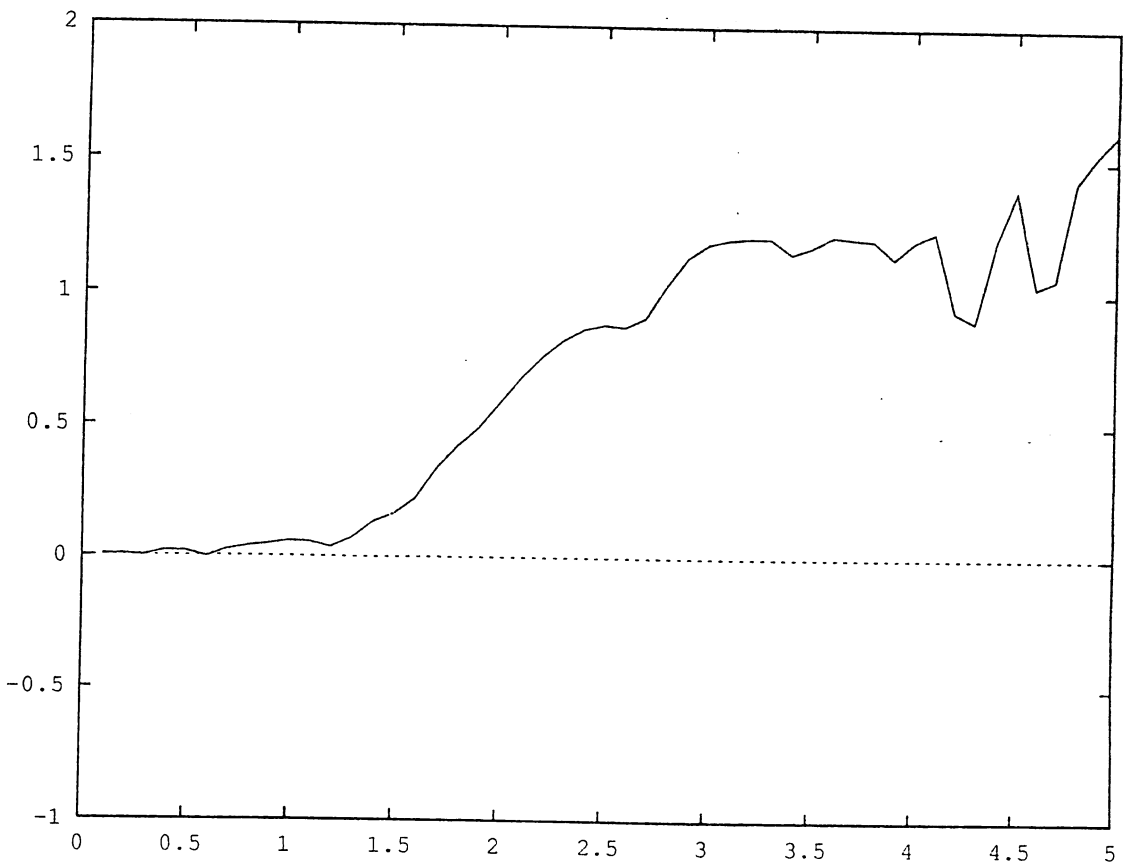

Figure 5. Dynamo growth rate as a function of flow parameter α, with other parameters fixed.

§4. Problems with Similar Structure

Problems with structure similar to the infinitely conducting dynamo problem occur in many disciplines. We shall present one problem that describes a plausible biological situation, the growth of an algae population in a heterogeneous environments. This problem was invented specifically to furnish a scalar analog to the dynamo problem, however, so no claims are made for its relevance to real algae populations. Looking at it from a slightly different perspective makes a connection with the thermodynamic formalism for dynamical systems, albeit a slightly different thermodynamic formalism from that developed by Ruelle [48] and others. The last problem considered is a matrix analog of the dynamo problem. This problem is derived from the dynamo problem, in fact, and is intended to illustrate what happens when cancellation is not a problem.

4.1. Algae population growth. Let us imagine that the domain D is a fishtank of water with algae suspended in it. Lamps are arranged around D so that some places are brightly lit, some dark, and others cosy and intimate. Loudspeakers project romantic music into some areas to encourage reproduction. Other areas get government messages encouraging responsible family planning. We assume that the algae density is low enough so that they influence neither the velocity field nor the reproductive behavior of their neighbors. We can therefore suppose that the rate of population increase at any given point is proportional to the population already there, with some proportionality factor depending on the light and sound levels.

Suppose that the combined effect of all these stimuli can be expressed by one reproductive speed function $R(\mathbf{x})$, which is the local rate of population growth per unit population per unit time. $R(\mathbf{x})$ will be positive if the ambience at $\mathbf{x}$ favors procreation. We also allow negative values of R if the discouraging factors at $\mathbf{x}$ outweigh the encouraging factors.

If there is no motion in the fluid, and the algae do not diffuse, the concentration $C(\mathbf{x}, t)$ of algae satisfies

$$\partial_t C = RC. \tag{4.1.1}$$

The solution to (4.1.1) is

$$C(\mathbf{x}, t) = C(\mathbf{x}, 0) \exp[tR(\mathbf{x})]$$

If the environment favors growth at $\mathbf{x}$, i.e. if $R(\mathbf{x}) > 0$, the local population density at $\mathbf{x}$ grows exponentially; if $R(\mathbf{x}) < 0$, the local population decays exponentially.

From a global point of view, we are interested in whether the total algae population grows exponentially in time. If R is smooth with bounded derivatives on D, so that R has a well defined maximum R_{max} on D, then

$$\int_D C(\mathbf{x}, t) d\mathbf{x} \sim s(t) \exp[tR_{max}]$$

as $t \to \infty$. Here $s(t)$ is some function for which $t^{-1} log|s(t)| \to 0$ as $t \to \infty$, with the rate of decay depending on the nature of $R(\mathbf{x})$ near the maximum. For example, if the maximum is taken at one point $\mathbf{x}_{max}$ in the interior of D, then

$$s(t) = (2\pi t)^{-3/2} \det[R''(\mathbf{x}_{max})]^{-1/2}$$

where R'' is the Hessian (second derivative) matrix of R. So if R is positive anywhere the total algae population grows. A cleaner way to express this is

$$\lim_{t\to\infty} t^{-1} log \left| \int_D C(\mathbf{x}, t) d\mathbf{x} \right| = R_{max}. \tag{4.1.2}$$

Real algae execute small random motions with respect to the fluid while they are being carried around. This is modelled by adding diffusion to (4.1.1) with coefficient κ, yielding the linear reaction-diffusion equation

$$\partial_t C = RC + \kappa \nabla^2 C. \tag{4.1.3}$$

This equation can be analyzed in limit of small κ using integrals over Wiener paths. When κ is small, the Wiener paths stay close to the 'classical' fluid particle trajectories, which are all fixed points in the absence of flow. Hence most of the algae growth is going to occur for Wiener paths that stay close to the point of maximum R. When R has a single quadratic maximum at the interior point $\mathbf{x}_{max}$, a stationary phase integration yields

$$\lim_{t\to\infty} t^{-1} log \left| \int_D C(\mathbf{x}, t) d\mathbf{x} \right| \approx R_{max} - (2\pi\kappa)^{-3/2} det[R''(\mathbf{x}_{max})]^{-1/2}. \tag{4.1.4}$$

Observe that (4.1.4) goes nicely to (4.1.2) in the limit $\kappa \to 0$.

The same result can be obtained from the eigenvalue problem

$$\lambda \hat{C} = R\hat{C} + \kappa \nabla^2 \hat{C} \tag{4.1.5}$$

by seeking an eigenfunction $\hat{C}(\mathbf{x})$ localized near $\mathbf{x}_{max}$. The eigenvalue problem for the diffusionless algae system,

$$\lambda \hat{C} = R\hat{C}, \tag{4.1.6}$$

has no eigenfunctions in the usual sense, but clearly $\delta(\mathbf{x} - \mathbf{x}_{max})$ is an eigendistribution belonging to the eigenvalue R_{max}.

Note that $R(\mathbf{x}_0)$ is actually an eigenvalue of (4.1.6) in the weak sense, with eigendistribution $\delta(\mathbf{x} - \mathbf{x}_0)$, for *any* point $\mathbf{x}_0$ in the interior of D. However, these values are not close to anything in the spectrum of the diffusive operator, no matter how small κ is. This is a warning that not all eigenvalues of the infinitely conducting dynamo problem may be relevant to the fast dynamo problem. The collapse of the Mather spectrum [43] of the nondiffusive magnetic field evolution equation has been observed by de la Llave [44].

If the fluid constituting D is in motion, the algae concentration satisfies

$$(\partial_t + \mathbf{u}\cdot\nabla)C = RC. \tag{4.1.7}$$

if the algae do not random-walk, and

$$(\partial_t + \mathbf{u}\cdot\nabla)C = RC + \kappa\nabla^2 C \tag{4.1.8}$$

if they do. The eigenvalue problems associated with (4.1.7) and (4.1.8) are

$$\lambda\hat{C} + \mathbf{u}\cdot\nabla\hat{C} = R\hat{C} \quad , \quad \lambda\hat{C} + \mathbf{u}\cdot\nabla\hat{C} = R\hat{C} + \kappa\nabla^2\hat{C}. \tag{4.1.9}$$

respectively.

Except for the fact that magnetic fields are vectors and algae concentrations are scalars, equations (4.1.7) and (4.1.8) are identical to the induction equations (2.3.1) and (2.1.1), respectively. We can therefore derive a scalar analogue of the Cauchy solution by integrating the non-diffusive equation (4.1.8) along fluid particle trajectories. If $C_0(\mathbf{x})$ is the initial algae concentration field, then

$$C(\mathbf{x},t) = C_0(\mathbf{X}(\mathbf{x},t|0))\exp\left(\int_0^t R(\mathbf{X}(\mathbf{x},t|s))ds\right). \tag{4.1.10}$$

We cannot make any precise statements about the algae population growth unless we know the trajectories explicitly. Some information may still be obtained by integrating various quantities over D. First, we assume the initial concentration $C_0(\mathbf{x})$ is everywhere positive, which makes sense for a density field. This implies that $C(\mathbf{x},t)$ will then be positive everywhere for all $t > 0$, whether or not diffusion is present.

If we integrate (4.1.10) over D, and apply Jensen's inequality [49] and some other standard inequalities, we obtain a lower bound:

$$\int_D C(\mathbf{x},t)d\mathbf{x} \geq V_D\left(\inf_{\mathbf{x}\in D} C_0(\mathbf{x})\right)\exp\left(tV_D^{-1}\int_D R(\mathbf{x}))d\mathbf{x}\right), \tag{4.1.11}$$

where V_D is the volume of D. Thus, a sufficient condition for exponential growth of the total algae population is that the integral of R over D be positive. This is a nice, simple condition. Nonetheless, this is a far weaker result than we have in the flow-free case. The problem is that (4.1.11) is the minimal result we can get without using information about the flow.

There is no Cauchy solution for the diffusive problem. But if the initial data for (4.1.10) is positive everywhere then we can write an equation for $S(\mathbf{x},t) \equiv \log C(\mathbf{x},t)$:

$$(\partial_t + \mathbf{u}\cdot\nabla)S = R + \kappa|\nabla S|^2 + \kappa\nabla^2 S. \tag{4.1.12}$$

Integrating (4.1.12) over space and time gives

$$\int_D S(\mathbf{x},t)d\mathbf{x} + \int_0^t\int_{\partial D}\mathbf{n}\cdot\mathbf{u}SdAdt - \int_D \log C_0(\mathbf{x})d\mathbf{x}$$

$$= t\int_D R(\mathbf{x})d\mathbf{x} + \int_0^t \int_D \kappa|\nabla S|^2 d\mathbf{x}dt + \int_0^t \int_{\partial D} \mathbf{n}\cdot\nabla S dA dt.$$

The surface integrals vanish if the boundaries of D are impermeable to algae and fluid, or if D has no boundary. The same inequalities as before imply that

$$\int_D C(\mathbf{x},t)dt \geq V_D\left(\inf_{\mathbf{x}\in D} C_0(\mathbf{x})\right)\exp\left(tV_D^{-1}\int_D R(\mathbf{x})d\mathbf{x}\right). \tag{4.1.13}$$

Again, positivity of $\int_D R(\mathbf{x})d\mathbf{x}$ is a sufficient condition for exponential growth of the total population. We remark that this result can also be obtained by expressing the solution to the diffusive initial-value problem as an integral over Wiener paths.

An upper bound on the exponential growth rate of the population can be obtained by multiplying either (4.1.7) or (4.1.8) by $C(\mathbf{x},t)$ and integrating over D. After integrating by parts and discarding the surface integrals, we obtain

$$\frac{d}{dt}\int_D C^2(\mathbf{x},t)d\mathbf{x} \leq 2\int_D R(\mathbf{x})C^2(\mathbf{x},t)d\mathbf{x} \leq 2R_{max}\int_D C^2(\mathbf{x},t)d\mathbf{x},$$

and hence

$$\int_D C^2(\mathbf{x},t)d\mathbf{x} \leq \exp(2R_{max}t)\int_D C_0^2(\mathbf{x})d\mathbf{x}.$$

Cauchy's inequality now implies that

$$\int_D C(\mathbf{x},t)d\mathbf{x} \leq \left[V_D\int_D C_0^2(\mathbf{x})d\mathbf{x}\right]^{1/2}\exp(R_{max}t) \tag{4.1.14}$$

The appearance of C_0 in (4.1.11), (4.1.13), and (4.1.14) is not essential. More compactly, we can say that

$$\sup_{\mathbf{x}\in D} R(\mathbf{x}) \geq \limsup_{t\to\infty} t^{-1}\log\left|\int_D C(\mathbf{x},t)d\mathbf{x}\right|$$

$$\geq \liminf_{t\to\infty} t^{-1}\log\left|\int_D C(\mathbf{x},t)d\mathbf{x}\right| \geq \int_D R(\mathbf{x})d\mathbf{x} \tag{4.1.15}$$

whether or not diffusion is present. It seems quite likely that the infimum and supremum limits in (4.1.15) should be the same. However, establishing such a result is a subtle problem requiring, so far, special properties of the flow [50].

For diffusive problems, (4.1.15) implies the existence of a real eigenvalue greater than or equal to $\int_D R(\mathbf{x})d\mathbf{x}$ regardless of how small the diffusivity is. This is exactly the kind of result we would like for the dynamo problem, but which cannot be obtained because of cancellation. If it were possible to use a geometry in which cancellation could be prevented, fast dynamos would be easy to obtain [28,29].

A closer connection between the algae problem and the dynamo problem can be made if we abandon our physical picture of a tank of algae and allow the 'reproduction' function R to take complex values. The 'concentration' field C then also becomes complex in general, and cancellation becomes possible between intimately mixed regions of C with different arguments. Unfortunately, the author is unaware of any results for the case of complex R that give any insight whatever into the dynamo problem.

4.2. Thermodynamic formalism. Various investigations in dynamical systems theory produce results and formulas amazingly similar to formulas appearing in statistical mechanics. Only slight generalizations are necessary to make the analogy essentially complete [48]. Once a dynamical systems problem has been cast into a thermodynamic form, the thermodynamic analogy makes available a large amount of insight and intuition in interpreting what would otherwise be enigmatic formulas. There is no unique way to define thermodynamic for dynamical systems, as different problems have different thermodynamic analogs. The thermodynamic formulation of the following problem leads to exactly the same equations that emerge from the algae tank, but of course their interpretation is quite different.

Suppose there is a smooth function $E(\mathbf{x})$ defined on D. By Birkhoff's theorem [51] the time-average of E along a particle trajectory,

$$\bar{E}(\mathbf{a}) = \lim_{t\to\infty} t^{-1} \int_0^t E(\mathbf{X}(\mathbf{a}, 0|s))ds$$

exists for almost all points $\mathbf{a}$. But Birkhoff's theorem says nothing about the rate at which the time averages converge. Global information about the rates can be found by considering the distribution of the integrals of E along all possible particle trajectories of duration t. The generating, or partition, function of this distribution is

$$Z_E(\beta, t) = \int_D \exp\left[-\beta \int_0^t E(\mathbf{X}(\mathbf{x}, t|s))ds\right] d\mathbf{x}. \tag{4.2.1}$$

What this generating function does is focus attention on trajectories on which the finite-time average deviates from the infinite-time average. As $t \to \infty$ the probability of large deviations goes to zero; this is just Birkhoff's theorem. But the contribution of deviations to the integral (4.2.1) may still be important because they are exponentiated. Just what the relative importance is depends on β. The β dependence of (4.2.1) encodes information about the deviations just as the ordinary generating function of a probability distribution encodes information about the distribution function. These considerations are the basis of large deviation theory [52,53].

Inspecting (4.2.1) indicates that $Z(\beta, t)$ probably increases or decreases exponentially with t. Furthermore, determining whether or not $Z_E(\beta, t)$ increases or decreases exponentially is exactly the same problem as determining whether the non-diffusing algae population will increase or decrease exponentially. The only difference is that (4.2.1) contains the tunable parameter β. If the exponential behavior is sufficiently well behaved, we can identify its growth rate as

$$\Lambda_E(\beta) = \lim_{t\to\infty} t^{-1} log Z_E(\beta, t) \tag{4.2.2}$$

The author is not sure what conditions on the flow or the function E guarantee the existence of this limit, but they are not expected to be very stringent. The growth rate bounds derived for the algae tank model imply that

$$-\beta V_D^{-1} \int_D E(\mathbf{x})d\mathbf{x} \leq \Lambda_E(\beta) \leq \sup_{\mathbf{x}\in D} (-\beta E(\mathbf{x})).$$

Equations (4.2.1) also suggests that Z_E depends exponentially on $-\beta$, so we define

$$F_E(\beta) = -\frac{1}{\beta}\Lambda_E(\beta) \tag{4.2.3}$$

Since the free energy of a thermodynamical system is defined by an almost identical formula [54], F_E is called the free energy at inverse temperature β.

The corresponding internal energy is defined by:

$$U_E(\beta) = -\frac{d}{d\beta}\Lambda_E(\beta), \tag{4.2.4}$$

$$= \lim_{t\to\infty} \frac{\int_D \left(t^{-1}\int_0^t E(\mathbf{X}(\mathbf{x},t|s))ds\right)\exp\left[-\beta\int_0^t E(\mathbf{X}(\mathbf{x},t|s))ds\right]d\mathbf{x}}{\int_D \exp\left[-\beta\int_0^t E(\mathbf{x},t|s)ds\right]d\mathbf{x}}.$$

The act of exchanging the limit as $t\to\infty$ and the β derivative is not strictly justified, of course. The internal energy has the simple interpretation of simply being a weighted average over D of finite-time time averages:

$$U_E(\beta) = \lim_{t\to\infty}\left\langle t^{-1}\int_0^t E(\mathbf{X}(\mathbf{x},t|s))ds\right\rangle_\beta$$

where the weight on the trajectory starting at $\mathbf{x}$ is

$$\exp\left[-\beta\int_0^t E(\mathbf{x},t|s)ds\right].$$

As mentioned before, it's not known under what circumstances these limits exist. However, if $\Lambda_E(\beta)$ exists for all β, and limit converges uniformly in β, then F_E and U_E are guaranteed to exist. We can differentiate again to get the specific heat

$$C_E(\beta) = -\beta^2\frac{d}{d\beta}U_E(\beta) = \beta^2\frac{d^2}{d\beta^2}\Lambda_E(\beta) \tag{4.2.5}$$

$$= \beta^2\lim_{t\to\infty}\left[\left\langle\left(t^{-1}\int_0^t E(\mathbf{X}(\mathbf{x},t|s))ds\right)^2\right\rangle_\beta - \left\langle t^{-1}\int_0^t E(\mathbf{X}(\mathbf{x},t|s))ds\right\rangle_\beta^2\right].$$

Just as in ordinary statistical mechanics, the specific heat measures mean square fluctuations, or variances.

It's a fundamental fact that variances are non-negative. Hence $\Lambda_E(\beta)$ is a convex function of β. However, it may not be strictly convex, if the averages converge so fast that the limiting variance (4.2.5) is zero. Alternatively, no one ever said the variance has to be finite either. An infinite variance means that the time-averages converge very slowly over some finite-measure set of points in D. When this happens, the graph of Λ_E develops a singularity in its second derivative. If the singularity is

weak the first derivative may be continuous, but a strong singularity will give a jump discontinuity in the first derivative of Λ_E, i.e. the internal energy U_E. The size of the jump is constrained by the fact that $U_E(\beta)$ always lies between the maximum and minimum values of E, and is monotonically increasing with β. An infinite specific heat indicates a phase transition in standard thermodynamics, so we shall call it a phase transition here too. When the flow is not ergodic, an infinite second derivative of Λ_E at $\beta = 0$ is expected on general grounds. However, the factor β^2 in (4.2.5) implies that this is not to be considered a phase transition in the usual sense.

The entropy belonging to this artificial thermodynamics is

$$S_E(\beta) = \beta(U_E(\beta) - F_E(\beta)) = \int_0^\beta \beta^{-1} C_E(\beta) d\beta. \tag{4.2.6}$$

As far as the author knows, there is no connection between this entropy and the various other entropies that can be defined for the flow considered as a dynamical system. Entropies tend to quantify the notion of disorder or lack of knowledge about the system. The appearance of the specific heat in (4.2.6) shows that the entropy measures the variances of the trajectory averages at all different temperatures, and integrates to get a global measure. Small entropy is associated with rapidly converging averages and the ability to get good information about the system with comparatively little data. Large entropy is associated with time averages which converge slowly, and the necessity of using large quantities of data to obtain information.

The problem of computing $\Lambda_E(\beta)$ can be cast as as eigenvalue problem on the space of scalar distributions on D. Specifically, the problem is to find eigendistributions $\hat{C}(\mathbf{x})$ and eigenvalues λ satisfying

$$\lambda \hat{C} + \mathbf{u} \cdot \nabla \hat{C} = \beta E \hat{C}$$

in the distributional sense. Provided the corresponding $\hat{C}$ returns something nonzero when applied to the smooth function 1, $\Lambda_E(\beta)$ will be the real part of the eigenvalue with largest real part. We anticipate, again without knowing any definite results, that $\Lambda_E(\beta)$ will be the limit as $\kappa \to 0+$ of the real part of the dominant eigenvalue of the diffusive problem

$$\lambda \hat{C} + \mathbf{u} \cdot \nabla \hat{C} = \beta E \hat{C} + \kappa \nabla^2 \hat{C}. \tag{4.2.7}$$

This diffusive problem has a nice interpretation of its own. If we think of the diffusion as being the result of noise continually perturbing the trajectories, the dominant eigenvalue of (4.2.7) is the starting point for the thermodynamic formalism of a noisy dynamical system. Now, a noisy dynamical system is a Markov system, and there is a great deal of theory in existence for large deviations in Markov systems [52].

Most of the nice results in thermodynamics and thermodynamic formalism apply to the case of real β, in which case there is no cancellation in the integral (4.2.1).

Cancellation problem could be studied with complex β. When β becomes complex, however, the function $\Lambda_E(\beta)$ is no longer convex in general, and may even vanish at certain values of β. Without convexity, the whole problem becomes extremely mysterious; it is unclear even what kind of analytical tools to bring to bear on the subject.

The algae tank and thermodynamic formalism problems can be formulated as pulsed flow problems for the purpose of computations. They become the same problem, in fact, if we identify $R(\mathbf{x})$ with $\beta E(\mathbf{x})$. If T represents the time-τ flow map, the Cauchy solution (4.1.10) for the algae problem yields a finite-time evolution equation for the fields $C_n(\mathbf{x}) = C(\mathbf{x}, n\tau)$:

$$C_{n+1}(\mathbf{x}) = \exp[\beta G(T^{-1}(\mathbf{x}))]C_n(T^{-1}(\mathbf{x})) = [\mathcal{M}_0 C_n](\mathbf{x}) \tag{4.2.8}$$

where $G(\mathbf{a})$ is the integral of E along the trajectory that starts at $\mathbf{a}$ and runs for time τ. Since E was introduced as just some arbitrary function of position, we lose no generality if we specify the function G as part of the computation instead of E. We use the symbol $\mathcal{M}_0$ to represent the time-τ evolution operator to emphasize the analogy with the dynamo problem.

Given the map T, a function G of position, and a parameter β, the recursion (4.2.8) can be simulated with exactly the same algorithm as was used for the dynamo simulations. We chose the same family of pulsed flows, except that the z-component of the flow and any possible z-dependence of the C-field were neglected. We took $\tau = 3$ in all the simulations reported in this section. Computations were performed with several different G functions, and

$$G(\mathbf{x}) = 1 + cos(y - \phi) - sin(x - \phi), \tag{4.2.9}$$

produced interesting results. The computations were done with $N = 256$ cells in each direction, in the square domain D used for the dynamo simulations.

First we set β to selected values and iterated the spatially discretized version of (4.2.8) until the growth rate had converged to within 10^{-4} and the spatial structure had converged to an eigenfunction of the discretized operator. Figure 6 shows the contours of $\log(\max(1, |\hat{C}(\mathbf{x})|)$ in the square $0 \leq x, y \leq 2\pi$, where $\hat{C}$ is the normalized eigenfunction, for two values of β. Figure 6a has $\beta = 1.$, and figure 6b has $\beta = i = \sqrt{-1}$.

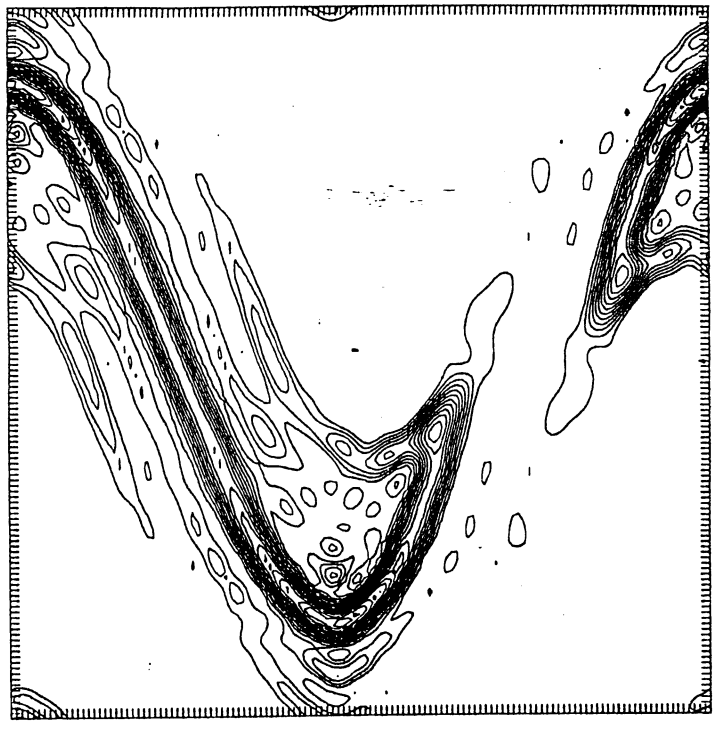

Figure 6a

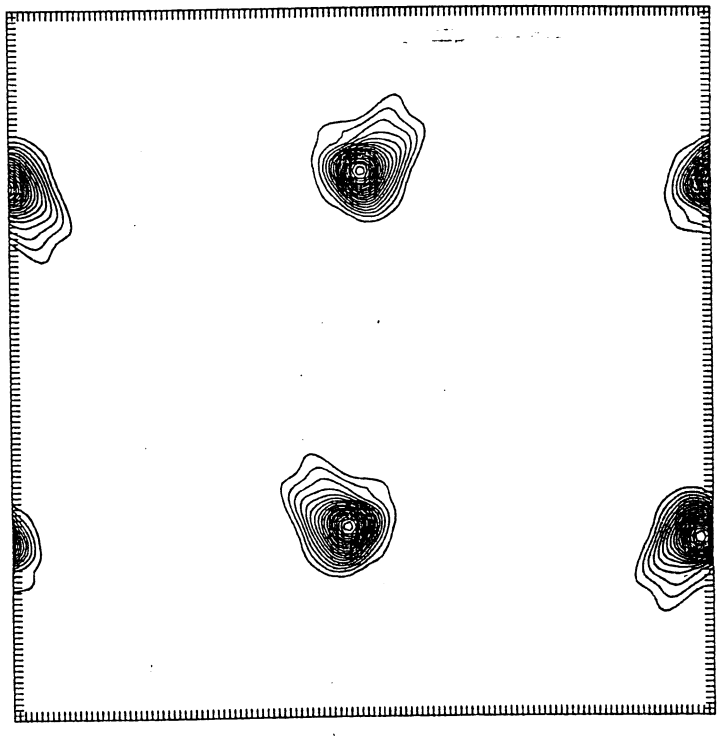

Figure 6b

Figure 6. Logarithmic contour plots of dominant eigenfunctions of algae tank or thermodynamic formalism operator. (a) corresponds to $\beta = 1$, (b) to $\beta = i$.

The extremely regular structure in figure 6b is not expected to occur for all choices of the function G when β is pure imaginary, but it does hint that problems involving complex 'temperatures' might not be completely intractable. The principle of stationary phase seems to underlie the regular structure seen here. Since the maximum and minimum values of this particular G function coincide with fixed points of the map T, there is very little complex phase mixing in the neighborhoods of these points. The places where the eigenfunction concentrates are the regions where phase cancellation is least effective. Although figure 6b is the result of a fairly contrived computation, this observation might give insight into more realistic situations.

Second, we computed the growth rate, defined as the natural logarithm of the asymptotic factor by which the field C_n is multiplied with every iteration of $\mathcal{M}_0$, as a function of real β between -5 and 5. This growth rate is $\Lambda_E(\beta)$, and is plotted in figure 7a. Once we have Λ_E, the other thermodynamic quantities can be found by differentiating Λ_E and multiplying by factors of β where indicated. Figure 7b shows the free energy as a function of β, figure 7c the internal energy, figure 7d the entropy, and figure 7e the specific heat. All these curves appear smooth, but the specific heat has two very pronounced peaks that might indicate a phase transition if the computations were done at higher resolution.

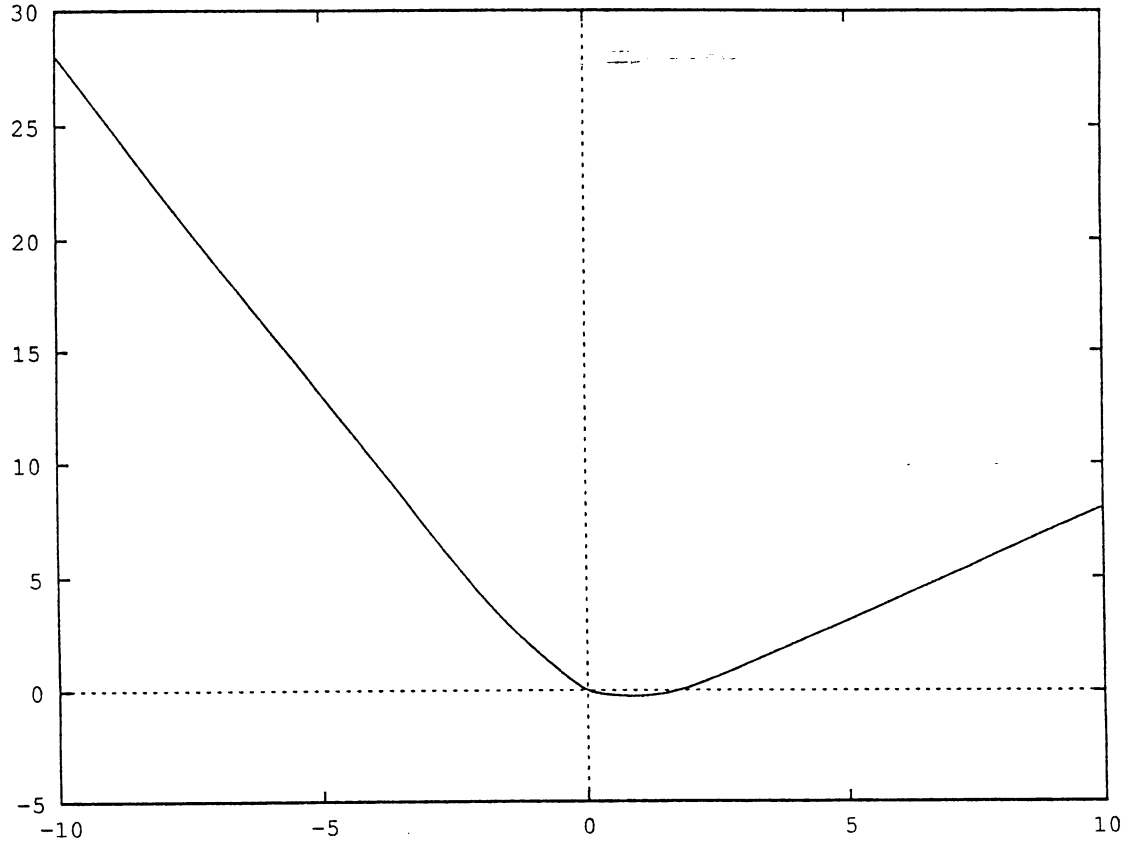

Figure 7a

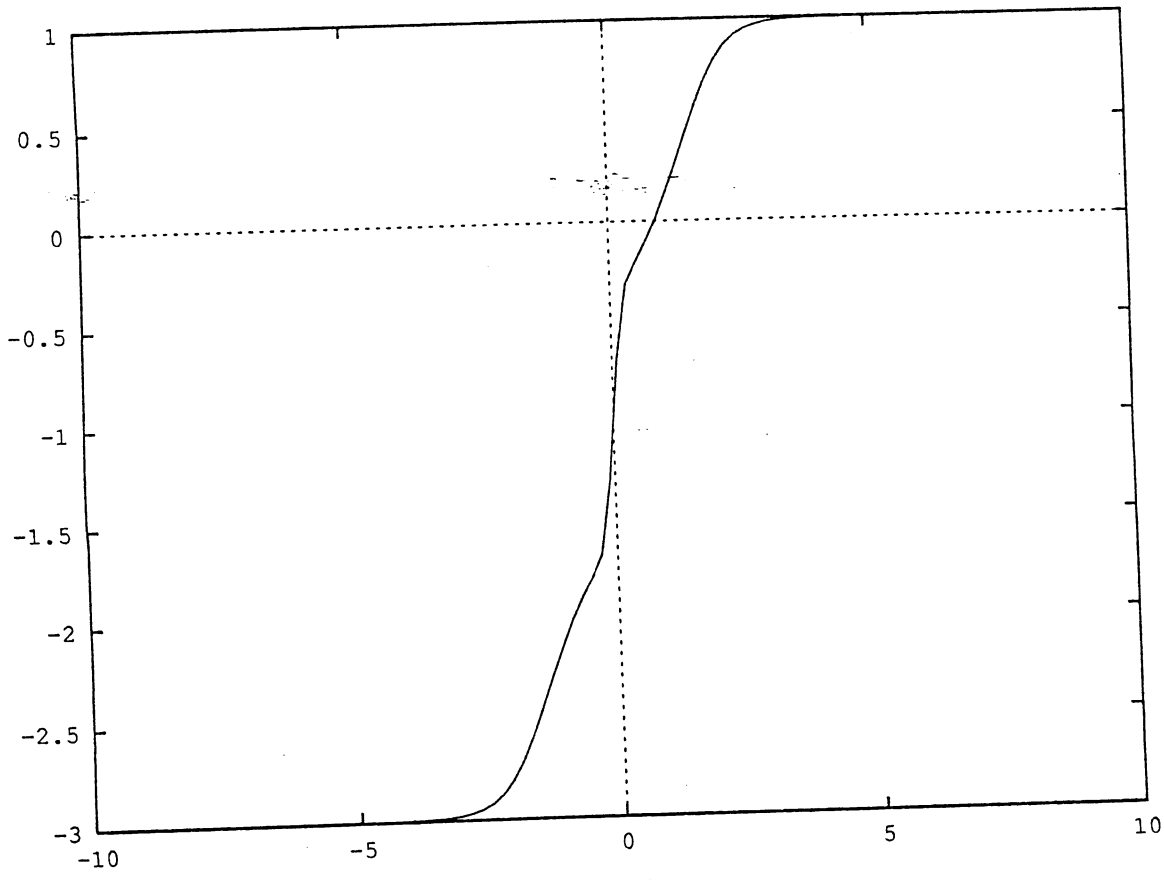

Figure 7b

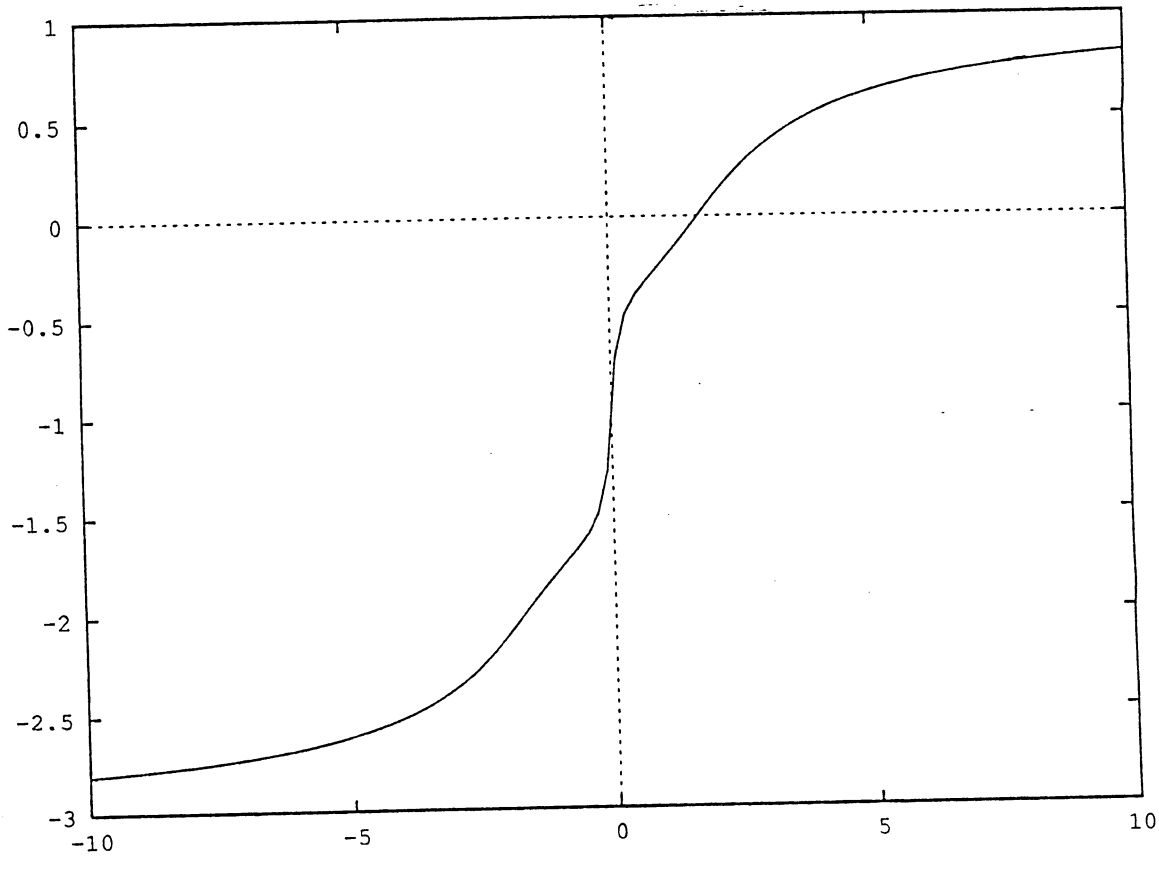

Figure 7c

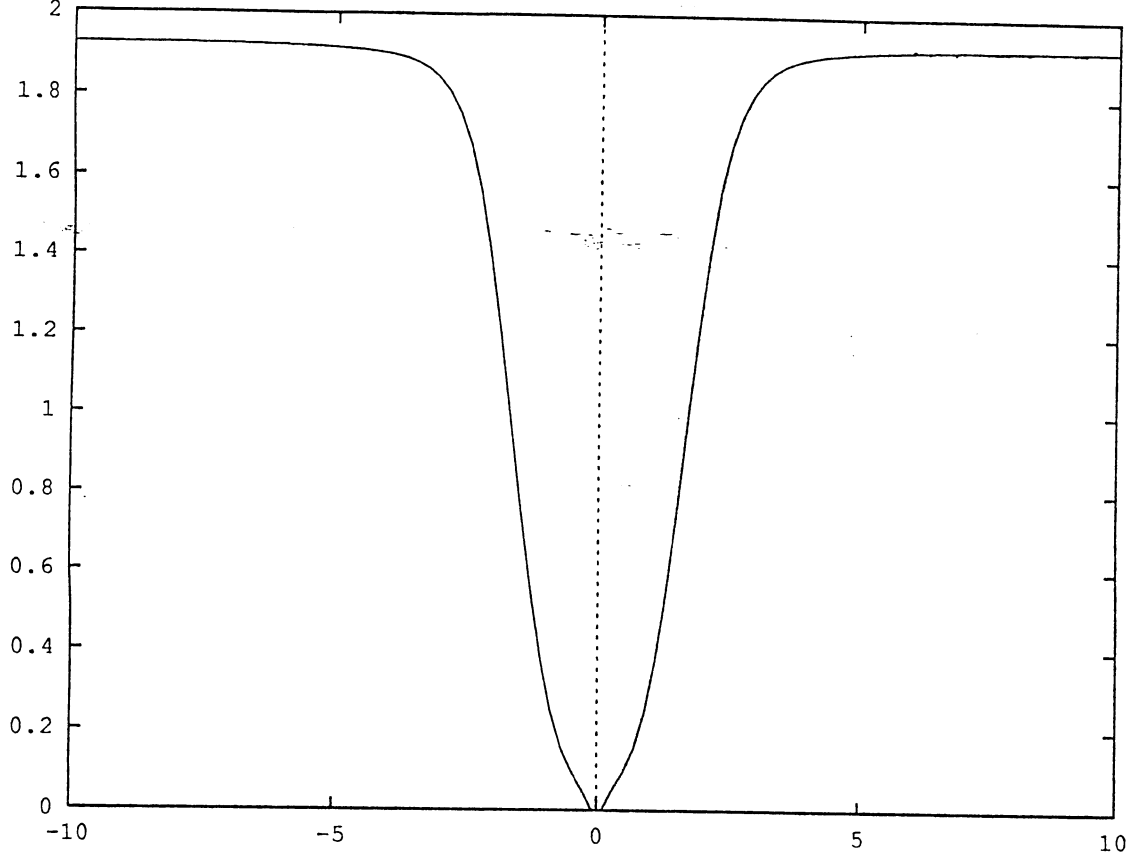

Figure 7d

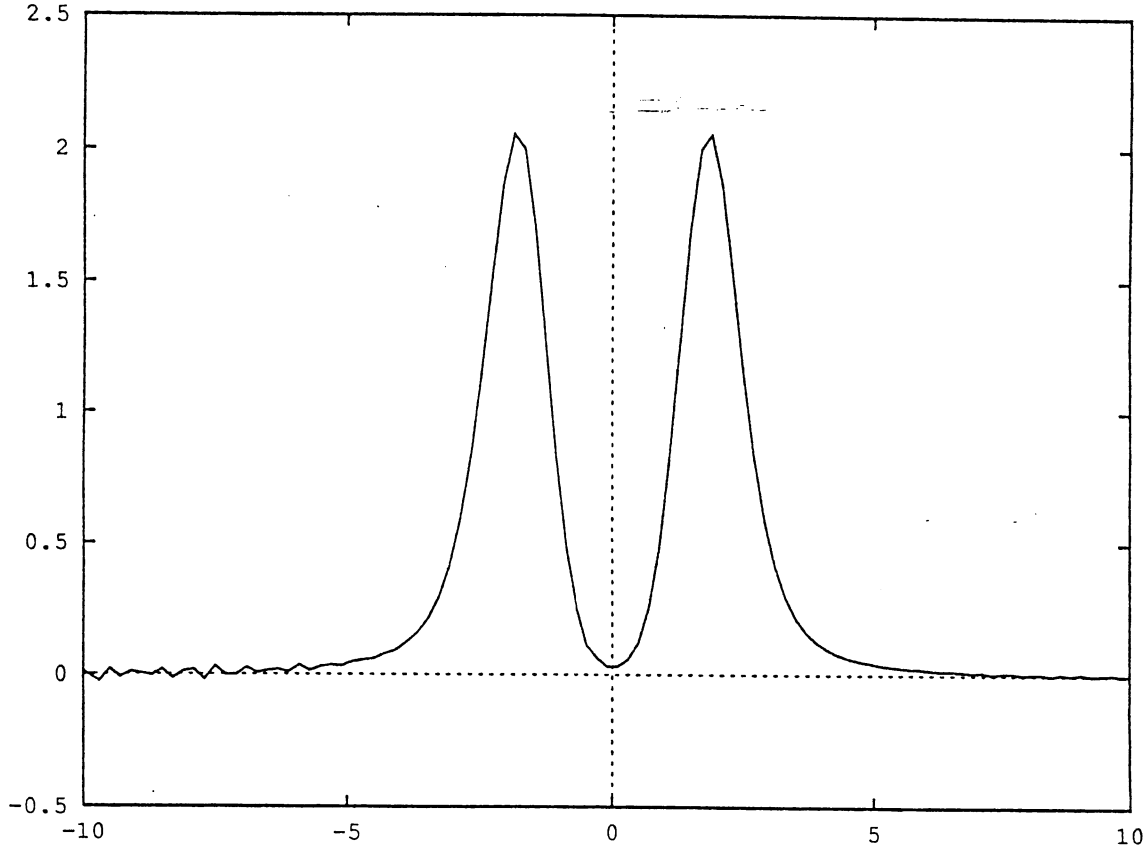

Figure 7e

Figure 7. Thermodynamic quantities as functions of β. (a) is $\Lambda_E(\beta)$, (b) is $F_E(\beta)$, (c) is $U_E(\beta)$, (d) is $S_E(\beta)$, and (e) is $C_E(\beta)$.

4.3. Quadratic form dynamo. We have looked briefly at the dynamo problem, which deals with vector fields, and two scalar problems which have similar structure. The scalar problems contained the functions $R(\mathbf{x})$ and $E(\mathbf{x})$, which were specified independently of the flowfield. Although of interesting structure, they are not completely relevant to the original dynamo problem. We next consider a problem in which the quantity of interest is a matrix-valued function.

Recall the non-diffusive magnetic induction equation (2.3.1). If $\mathbf{B}$ is specified at $t = 0$, the subsequent evolution is given by the Cauchy formula (2.3.4). The problem in determining whether we have an infinitely conducting dynamo is cancellation. One possible way to avoid cancellation would be to square the field, so that we never have quantities of opposite sign in close proximity. For a vector quantity like magnetic field, a sensible way to square the field is to form the square matrix

$$\mathbf{Q}(\mathbf{x},t) = \mathbf{B}(\mathbf{x},t)\mathbf{B}^T(\mathbf{x},t) \tag{4.3.1}$$

So defined, $\mathbf{Q}(\mathbf{x},t)$ is symmetric and positive-semi-definite. Also, if $\mathbf{B}(\mathbf{x},t)$ evolves according to (2.3.1), then

$$(\partial_t + \mathbf{u}\cdot\nabla)\mathbf{Q} = [\nabla\mathbf{u}]\mathbf{Q} + \mathbf{Q}^T[\nabla\mathbf{u}]^T. \tag{4.3.2}$$

However, not every solution of (4.3.2) is the external square of a vector field. We could take any initial $\mathbf{Q}$ field consisting of symmetric positive-semi-definite or positive-definite matrices, and let it evolve according to (4.3.2). As in the preceding problems, we want to know if $\mathbf{Q}$ increases exponentially as $t \to \infty$. We expect that this kind of statement will make sense only in the sense of distributions, so the appropriate question to ask is whether

$$\int_D trace[\mathbf{A}(\mathbf{x})\mathbf{Q}(\mathbf{x},t)]d\mathbf{x}$$

increases exponentially with time, for some smooth matrix-valued function $\mathbf{A}(\mathbf{x})$ and smooth initial $\mathbf{Q}$ field.

Diffusion can be added formally to (4.3.2), yielding

$$(\partial_t + \mathbf{u}\cdot\nabla)\mathbf{Q} = [\nabla\mathbf{u}]\mathbf{Q} + \mathbf{Q}^+[\nabla\mathbf{u}]^+ + \varepsilon\nabla^2\mathbf{Q}. \tag{4.3.3}$$

Note that (4.3.3) is not the equation for the tensor square of the solution to the diffusive induction equation (2.1.1). It can be shown that a sufficient condition for exponential growth of solutions to (4.3.2) is for the flow to be Anosov. The argument is essentially the same as that given by Bayly [28] and Vishik [29], except that no orientability condition is required on the dilating or contracting direction fields. Our numerical results suggest that any degree of Lagrangian chaos guarantees exponential growth in (4.3.2) and also (4.3.3). Indeed, the growth rate is expected to exceed

$$V_D^{-1}\int_D \lambda_{\mathbf{u}}(\mathbf{a})d\mathbf{a}$$

by a Jensen's inequality argument similar to that used in the algae problem. This bound is expected to hold for small positive values of κ also.

Again, it is straightforward to simulate (4.3.2) using the same technique as in the dynamo and algae problems. Since no matrix antidynamo theorems force us to work in three dimensions, we let the problem be purely two-dimensional. Figure 8 shows a contour plot of $\log(\max(1, |Q(\mathbf{x})|))$ in the domain D; here $|\mathbf{Q}|$ denotes the sum of the absolute values of the elements of $\mathbf{Q}$. Figure 9 shows the growth rate as a function of α. Note that the growth rate is always slightly greater than α, in contrast to the same plot for the ordinary vector dynamo in which the growth rate is always much less than α. This reveals that even though perfect cancellation can be avoided in three dimensions, we can expect extremely good cancellation unless a system is specifically constructed to have zero cancellation.

§5. Discussion

The dynamo problem has been around for a long time. One reason it has been around so long is that as progress is made, the problem changes. Like heads of the Hydra, when one version of the dynamo problem is solved, another grows in its place. The fast dynamo problem was identified by Vainshtein and Zeldovich [17] in 1972.

The last few years have seen significant progress. Theoretical and numerical investigations have progressed hand-in-hand, each guiding the other. We now have a good idea of what a fast dynamo is and what kinematic properties of a flow seem to be favorable or unfavorable for a fast dynamo. The problem now is *proving* that some likely candidate really is a fast dynamo. This is not proof in the rigorous sense of pure mathematics. What we are looking for is some quantitative argument that explicitly considers the problem of the arbitrarily small-scale structure that develops as the diffusivity goes to zero, and shows that the development of the small scale structure is consistent with growth of the field as a whole.

An asymptotic theory in the limit $\varepsilon \to 0$ would be wonderful. However, asymptotic expansions seem to be available only when the flow is regular in structure, and integrable [15,16,27]. It is difficult to say where the diffusive or boundary layers are likely to occur in the absence of generalized coordinates whose surfaces give the loci of the singular layers. Numerical computations do a good job of showing what happens at small finite diffusivity and large, finite numerical resolution. If we were doing a problem with a smooth solution, we could justify the results using either local asymptotic error analysis [41] or possibly even a computer-assisted proof [55-57]. But here we are discretizing a problem whose continuous version has a solution which may be nowhere smooth, or even finite.

Another possibility is that a problem equivalent to the fast dynamo problem may have been solved in some other discipline. The author has not yet found a discipline in which the fast dynamo problem has been solved, but there are plenty of other disciplines containing problems similar to the fast dynamo problem. A prominent example is thermodynamic formalism for dynamical systems, which is itself contained within large-deviation theory. But large-deviation theory is mostly

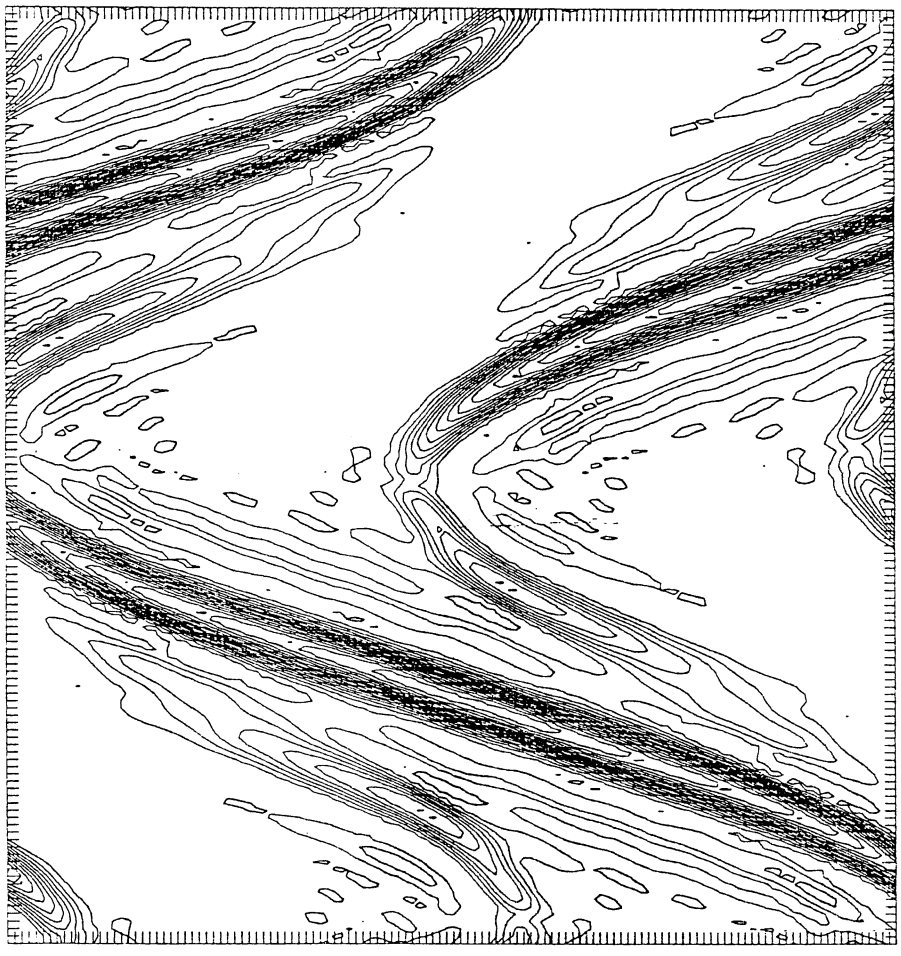

Figure 8. Logarithmic contour plot of dominant eigenfunction of quadratic form dynamo, at resolution $N = 128$.

concerned with the distribution of sums of random scalars, while the fast dynamo problem is concerned with the distribution of products of random matrices. Also, large-deviation theory is mostly concerned with real scalars, so that information about problems involving cancellation is slight.

This lecture has described the fast dynamo problem and a few other problems with similar structure. They are difficult to analyze, but it is hard to believe they're

too complex to be understood in simple terms. Once the right insight is found, they should tumble like dominoes, and we will suddenly know much more about some very interesting problems.

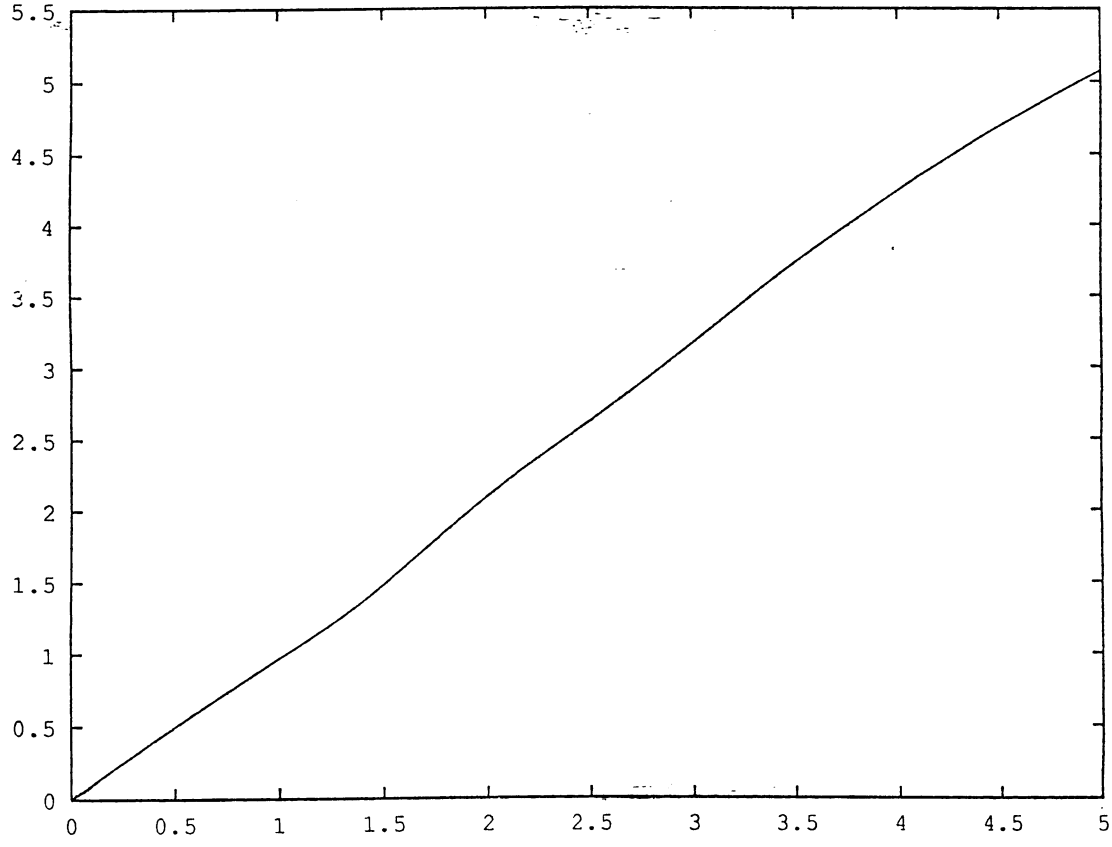

Figure 9. Quadratic form dynamo growth rate as a function of α.

ACKNOWLEDGMENTS

The author has discussed the fast dynamo problem with many scientists, and received valuable feedback from many different directions. He would like to acknowledge in particular Jim Shearer, Alp Eden, Rafael de la Llave, David Levermore, Robert Maier, Lai-Sang Young, Andrew Gilbert, Isaac Klapper, Mikhail Vishik, Alexander Ruzmaikin, and John Finn. The work grew out of a collaboration with Steve Childress, who is the primary source of many of the ideas presented here. The computations were performed on the CONVEX machines at the University of Arizona.

REFERENCES

[1] H.K. MOFFATT, *Magnetic Field Generation in Electrically Conducting Fluids*, Cambridge University Press, 1978.
[2] E.N. PARKER, *Cosmical Magnetic Fields*, Oxford University Press, 1979.
[3] J.A. JACOBS (ED.), *Geomagnetism*, Academic Press, 1989.
[4] A.M. SOWARD (ED.), *Stellar and Planetary Magnetism*, Gordon and Breach Science Publishers, 1983.
[5] E.R. PRIEST, *Solar Magnetohydrodynamics*, D. Reidel, 1982.
[6] D. GUBBINS, *Energetics of the Earth's core*, J. Geophysics, 43 (1977), p. 453.
[7] D.O. GOUGH AND N.O. WEISS, *The calibration of stellar convection theories*, Mon. Not. Roy. Astron. Soc., 176 (1976), p. 589.

[8] T.G. COWLING, *The magnetic field of sunspots*, Mon. Not. Roy. Astron. Soc., 94 (1934), p. 39.

[9] YA. B. ZEL'DOVICH, *The magnetic field in the two-dimensional motion of a conducting turbulent fluid*, Sov. Phys. JETP, 4 (1957), p. 460.

[10] A. HERZENBERG, *Geomagnetic dynamos*, Phil. Trans. Roy. Soc. A, 250 (1958), p. 543.

[11] G. E. BACKUS, *A class of self-sustaining dissipative spherical dynamos*, Ann. Physics, 4 (1958), p. 372.

[12] M. STEENBECK, F. KRAUSE, AND K.-H. RÄDLER, *The generation of magnetic fields by turbulent dynamo action*, Z. Naturforsch., 21a (1966), p. 21; English translation: NCAR Tech. Note 60 by P.H. Roberts and M. Stix, (1971).

[13] P. H. ROBERTS, *From Taylor state to Model-Z?*, Geophys. Astrophys. Fluid Dynamics, 49 (1989), p. 143.

[14] G.O. ROBERTS, *Dynamo action of fluid motions with two-dimensional periodicity*, Phil. Trans. Roy. Soc. A, 271 (1972), p. 411.

[15] S. CHILDRESS, *Alpha-effect in flux ropes and sheets*, Phys. Earth Planet. Interiors, 20 172 (1979).

[16] A.M. SOWARD AND S. CHILDRESS, *Analytic theory of dynamos*, Advances in Space Research, 6 (1986), p. 7.

[17] S.I. VAINSHTEIN AND YA. B. ZEL'DOVICH, *Origin of magnetic fields in astrophysics*, Sov. Phys. Usp., 15 (1972), p. 159.

[18] V.I. ARNOL'D, YA.B. ZEL'DOVICH, A.A. RUZMAIKIN, AND D.D. SOKOLOV, *A magnetic field in a stationary flow with stretching in Riemannian space*, Sov. Phys. JETP, 54 (1981), p. 1083.

[19] B.J. BAYLY AND S. CHILDRESS, *Fast dynamo action in unsteady flows and maps in three dimensions*, Phys. Rev. Letters, 59 (1987), p. 1573.

[20] J.M. FINN AND E. OTT, *Chaotic flows and fast magnetic dynamos*, Phys. Rev. Letters, 60 (1988), p. 760.

[21] H.R. STRAUSS, *Resonant fast dynamo*, Phys. Rev. Letters, 57 (1986), p. 2231.

[22] V.I. ARNOL'D AND E.I. KORKINA, *The growth of a magnetic field in a three-dimensional steady incompressible flow*, Vestnik Moscow State Univ., N3 (1983), p. 43.

[23] D. GALLOWAY AND U. FRISCH, *Dynamo action in a family of flows with chaotic streamlines*, Geophys. Astrophys. Fluid Dynamics, 36 (1986), p. 58.

[24] B.J. BAYLY AND S. CHILDRESS, *Construction of fast dynamos using unsteady flows and maps in three dimensions*, Geophys. Astrophys. Fluid Dynamics, 44 (1988), p. 211.

[25] J.M. FINN AND E. OTT, *Chaotic flows and fast magnetic dynamos*, Phys. Fluids, 31 (1988), p. 2992.

[26] N.F. OTANI, *Computer Simulation of Fast Kinematic Dynamos*, EOS Transactions, American Geophysical Union 64, 44 (1988), p. 1366.

[27] A.M. SOWARD, *Fast dynamo action in a steady flow*, J. Fluid Mech, 180 (1987), p. 267.

[28] B.J. BAYLY, *Fast magnetic dynamos in chaotic flows*, Phys. Rev. Letters 57 (1986), p. 2800.

[29] M.M. VISHIK, *Magnetic field generation by the motion of a highly conducting fluid*, Geophys. Astrophys. Fluid Dynamics, 48 (1989), p. 151.

[30] J. PLANTE AND W. THURSTON, *Anosov flows and the fundamental group*, Topology, 11 (1972), p. 147.

[31] I. KLAPPER, PH.D. THESIS, COURANT INSTITUTE OF MATHEMATICAL SCIENCES.

[32] G.H. GOLUB AND C.F. VAN LOAN, *Matrix Computations*, Johns Hopkins University Press, 1983.

[33] I. GOLDHIRSCH, B. MAULIK, AND S.A. ORSZAG, *An efficient method for computing leading eigenvalues and eigenvectors of large asymmetric matrices*, J. Sci. Comput., 2 (1987), p. 33,.

[34] G.K. BATCHELOR, *An Introduction to Fluid Dynamics*, Cambridge University Press, 1967.

[35] H.K. MOFFATT AND M.R.E. PROCTOR, *Topological constraints associated with fast dynamo action*, J. Fluid Mech., 154 (1985), p. 493.

[36] R.H. KRAICHNAN, *Lagrangian velocity covariance in helical turbulence*, J. Fluid Mech., 81 (1977), p. 385.

[37] V.I. OSELEDEC, *A multiplicative ergodic theorem*, Trans. Moscow Math. Soc., 19 (1968), p. 197.

[38] B.J. BAYLY AND S. CHILDRESS, *Unsteady dynamo effects at large magnetic Reynolds number*, Geophys. Astrophys. Fluid Dynamics, 49 (1989), p. 23.

[39] D. GOTTLIEB AND S.A. ORSZAG, *Numerical Analysis of Spectral Methods*, SIAM Press, Philadelphia, 1977.

[40] R. COURANT, K.O. FRIEDRICHS, AND M. LEWY, *Über die partiallen differenzengleichungen der mathematische physik*, Math. Ann., 100 (1928), p. 32; *On the partial difference equations of mathematical physics*, English translation:, IBM J. Res. Devel., 11 (1967), p. 215.

[41] R. PEYRET AND T.D. TAYLOR, *Computational Methods for Fluid Flow*, Springer-Verlag, 1983.

[42] M. REED AND B. SIMON, *Methods of Modern Mathematical Physics, vol. 1: Functional Analysis*, Academic Press, 1980.

[43] J. MATHER, *Characterization of Anosov Diffeomorphisms*, Indag. Math., 30 (1968), p. 479.

[44] R. DE LA LLAVE, *Characterizations of hyperbolic sets and applications to fast dynamo theory*, preprint.

[45] V.I. ARNOL'D, *Sur la topologie des écoulements stationnaires des fluides parfaits*, C. R. Acad. Sci. Paris, 261 (1965), p. 17.

[46] T. DOMBRE, U. FRISCH, J.M. GREENE, M. HENON, A. MEHR, AND A.M. SOWARD, *Chaotic streamlines in the ABC flows*, J. Fluid Mech., 167 (1986), p. 353.

[47] A.D. GILBERT AND B.J. BAYLY, *Magnetic field intermittency and fast dynamo action in random helical flows*, submitted, J. Fluid Mech. (1990).

[48] D. RUELLE, *Thermodynamic Formalism*, Addison-Wesley, 1978.

[49] W. RUDIN, *Principles of Mathematical Analysis*, McGraw-Hill, 1976.

[50] L.-S. YOUNG, *Large deviations results for dynamical systems*, Trans. A.M.S., 318 (1990), p. 525.

[51] P.R. HALMOS, *Lectures on Ergodic Theory*, Chelsea Publishing Co., 1956.

[52] S.R.S. VARADHAN, *Large Deviations and Applications*, SIAM Press, 1984.

[53] R. ELLIS, *Entropy, Large Deviations, and Statistical Mechanics*, Springer-Verlag, 1985.

[54] K. HUANG, *Statistical Mechanics*, Wiley, 1963.

[55] C. FEFFERMAN AND R. DE LA LLAVE, *Relativistic stability of matter I*, Rev. Mat. Iber., 2 (1986), p. 119.

[56] M.T. NAKAO, *A computational verification method of existence for nonlinear elliptic equations*, in *Lecture Notes in Num. Appl. Anal.*, 1989, p. 101.

[57] K.R. MEYER AND D. SCHMIDT (ED.), *Computer Aided Proofs in Analysis*, Springer-Verlag, 1991.

Recent IMA Preprints

#	Author/s Title
801	**Hi Jun Choe**, Regularity for solutions of nonlinear variational inequalities with gradient constraints
802	**Peter Shi and Yongzhi Xu**, Quasistatic linear thermoelasticity on the unit disk
803	**Satyanad Kichenassamy and Peter J. Olver**, Existence and non-existence of solitary wave solutions to higher order model evolution equations
804	**Dening Li**, Regularity of solutions for a two-phase degenerate Stefan Problem
805	**Marek Fila, Bernhard Kawohl and Howard A. Levine**, Quenching for quasilinear equations
806	**Yoshikazu Giga, Shun'ichi Goto and Hitoshi Ishii**, Global existence of weak solutions for interface equations coupled with diffusion equations
807	**Mark J. Friedman and Eusebius J. Doedel**, Computational methods for global analysis of homoclinic and hetero clinic orbits: a case study
808	**Mark J. Friedman**, Numerical analysis and accurate computation of heteroclinic orbits in the case of center manifolds
809	**Peter W. Bates and Songmu Zheng**, Inertial manifolds and inertial sets for the phase-field equations
810	**J. López Gómez, V. Márquez and N. Wolanski**, Global behavior of positive solutions to a semilinear equation with a nonlinear flux condition
811	**Xinfu Chen and Fahuai Yi**, Regularity of the free boundary of a continuous casting problem
812	**Eden, A., Foias, C., Nicolaenko, B. and Temam, R.**, Inertial sets for dissipative evolution equations Part I: Construction and applications
813	**Jose–Francisco Rodrigues and Boris Zaltzman**, On classical solutions of the two-phase steady-state Stefan problem in strips
814	**Viorel Barbu and Srdjan Stojanovic**, Controlling the free boundary of elliptic variational inequalities on a variable domain
815	**Viorel Barbu and Srdjan Stojanovic**, A variational approach to a free boundary problem arising in electro-photography
816	**B.H. Gilding and R. Kersner**, Diffusion-convection-reaction, free boundaries, and an integral equation
817	**Shoshana Kamin, Lambertus A. Peletier and Juan Luis Vazquez**, On the Barenblatt equation of elasto-plastic filtration
818	**Avner Friedman and Bei Hu**, The Stefan problem with kinetic condition at the free boundary
819	**M.A. Grinfeld**, The stress driven instabilities in crystals: mathematical models and physical manifestations
820	**Bei Hu and Lihe Wang**, A free boundary problem arising in electrophotography: solutions with connected toner region
821	**Yongzhi Xu, T. Craig Poling, and Trent Brundage**, Direct and inverse scattering of time harmonic acoustic waves in an inhomogeneous shallow ocean
822	**Steven J. Altschuler**, Singularities of the curve shrinking flow for space curves
823	**Steven J. Altschuler and Matthew A. Grayson**, Shortening space curves and flow through singularities
824	**Tong Li**, On the Riemann problem of a combustion model
825	**L.A. Peletier & W.C. Troy**, Self-similar solutions for diffusion in semiconductors
826	**C.J. van Duijn, L.A. Peletier & R.J. Schotting**, On the analysis of brine transport in porous media
827	**Minkyu Kwak**, Finite dimensional description of convective reaction-diffusion equations
828	**Minkyu Kwak**, Finite dimensional inertial forms for the 2D Navier–Stokes equations
829	**Victor A. Galaktionov and Sergey A. Posashkov**, On some monotonicity in time properties for a quasilinear parabolic equation with source
830	**Victor A. Galaktionov**, Remark on the fast diffusion equation in a ball
831	**Hi Jun Choe and Lihe Wang**, A regularity theory for degenerate vector valued variational inequalities
832	**Vladimir I. Oliker and Nina N. Uraltseva**, Evolution of nonparametric surfaces with speed depending on curvature, II. The mean curvature case.
833	**S. Kamin and W. Liu**, Large time behavior of a nonlinear diffusion equation with a source
834	**Shoshana Kamin and Juan Luis Vazquez**, Singular solutions of some nonlinear parabolic equations
835	**Bernhard Kawohl and Robert Kersner**, On degenerate diffusion with very strong absorption
836	**Avner Friedman and Fernando Reitich**, Parameter identification in reaction-diffusion models
837	**E.G. Kalnins, H.L. Manocha and Willard Miller, Jr.**, Models of q-algebra representations I. Tensor products of special unitary and oscillator algebras
838	**Robert J. Sacker and George R. Sell**, Dichotomies for linear evolutionary equations in Banach spaces
839	**Oscar P. Bruno and Fernando Reitich**, Numerical solution of diffraction problems: a method of variation of boundaries
840	**Oscar P. Bruno and Fernando Reitich**, Solution of a boundary value problem for Helmholtz equation via variation of the boundary into the complex domain
841	**Victor A. Galaktionov and Juan L. Vazquez**, Asymptotic behaviour for an equation of superslow diffusion. The Cauchy problem
842	**Josephus Hulshof and Juan Luis Vazquez**, The Dipole solution for the porous medium equation in several

space dimensions

843 **Shoshana Kamin and Juan Luis Vazquez**, The propagation of turbulent bursts

844 **Miguel Escobedo, Juan Luis Vazquez and Enrike Zuazua**, Source-type solutions and asymptotic behaviour for a diffusion-convection equation

845 **Marco Biroli and Umberto Mosco**, Discontinuous media and Dirichlet forms of diffusion type

846 **Stathis Filippas and Jong-Shenq Guo**, Quenching profiles for one-dimensional semilinear heat equations

847 **H. Scott Dumas**, A Nekhoroshev-like theory of classical particle channeling in perfect crystals

848 **R. Natalini and A. Tesei**, On a class of perturbed conservation laws

849 **Paul K. Newton and Shinya Watanabe**, The geometry of nonlinear Schrödinger standing waves

850 **S.S. Sritharan**, On the nonsmooth verification technique for the dynamic programming of viscous flow

851 **Mario Taboada and Yuncheng You**, Global attractor, inertial manifolds and stabilization of nonlinear damped beam equations

852 **Shigeru Sakaguchi**, Critical points of solutions to the obstacle problem in the plane

853 **F. Abergel, D. Hilhorst and F. Issard-Roch**, On a dissolution-growth problem with surface tension in the neighborhood of a stationary solution

854 **Erasmus Langer**, Numerical simulation of MOS transistors

855 **Haïm Brezis and Shoshana Kamin**, Sublinear elliptic equations in $\mathbb{R}^n$

856 **Johannes C.C. Nitsche**, Boundary value problems for variational integrals involving surface curvatures

857 **Chao–Nien Chen**, Multiple solutions for a semilinear elliptic equation on $\mathbb{R}^N$ with nonlinear dependence on the gradient

858 **D. Brochet, X. Chen and D. Hilhorst**, Finite dimensional exponential atttractor for the phase field model

859 **Joseph D. Fehribach**, Mullins-Sekerka stability analysis for melting-freezing waves in helium-4

860 **Walter Schempp**, Quantum holography and neurocomputer architectures

861 **D.V. Anosov**, An introduction to Hilbert's 21st problem

862 **Herbert E Huppert and M Grae Worster**, Vigorous motions in magma chambers and lava lakes

863 **Robert L. Pego and Michael I. Weinstein**, A class of eigenvalue problems, with applications to instability of solitary waves

864 **Mahmoud Affouf**, Numerical study of a singular system of conservation laws arising in enhanced oil reservoirs

865 **Darin Beigie, Anthony Leonard and Stephen Wiggins**, The dynamics associated with the chaotic of tangles two dimensional quasiperiodic vector fields: theory and applications

866 **Gui–Qiang Chen and Tai–Ping Liu**, Zero relaxation and dissipation limits for hyperbolic conservation laws

867 **Gui–Qiang Chen and Jian–Guo Liu**, Convergence of second–order schemes for isentropic gas dynamics

868 **Aleksander M. Simon and Zbigniew J. Grzywna**, On the Larché–Cahn theory for stress-induced diffusion

869 **Jerzy Łuczka, Adam Gadomski and Zbigniew J. Grzywna**, Growth driven by diffusion

870 **Mitchell Luskin and Tsorng-Whay Pan**, Nonplanar shear flows for nonaligning nematic liquid crystals

871 **Mahmoud Affouf**, Unique global solutions of initial-boundary value problems for thermodynamic phase transitions

872 **Richard A. Brualdi, Keith L. Chavey and Bryan L. Shader**, Rectangular L-matrices

873 **Xinfu Chen, Avner Friedman and Bei Hu**, The thermistor problem with zero–one conductivity II

874 **Raoul LePage**, Controlling a diffusion toward a large goal and the Kelly principle

875 **Raoul LePage**, Controlling for optimum growth with time dependent returns

876 **Marc Hallin and Madan L. Puri**, Rank tests for time series analysis a survey

877 **V.A. Solonnikov**, Solvability of an evolution problem of thermocapillary convection in an infinite time interval

878 **Horia I. Ene and Bogdan Vernescu**, Viscosity dependent behaviour of viscoelastic porous media

879 **Kaushik Bhattacharya**, Self-accommodation in martensite

880 **D. Lewis, T. Ratiu, J.C. Simo and J.E. Marsden**, The heavy top: a geometric treatment

881 **Leonid V. Kalachev**, Some applications of asymptotic methods in semiconductor device modeling

882 **David C. Dobson**, Phase reconstruction via nonlinear least-squares

883 **Patricio Aviles and Yoshikazu Giga**, Minimal currents, geodesics and relaxation of variational integrals on mappings of bounded variation

884 **Patricio Aviles and Yoshikazu Giga**, Partial regularity of least gradient mappings

885 **Charles R. Johnson and Michael Lundquist**, Operator matrices with chordal inverse patterns

886 **B.J. Bayly**, Infinitely conducting dynamos and other horrible eigenproblems

887 **Charles M. Elliott and Stefan Luckhaus**, 'A generalised diffusion equation for phase separation of a multi-component mixture with interfacial free energy'

888 **Christian Schmeiser and Andreas Unterreiter**, The derivation of analytic device models by asymptotic methods

889 **LeRoy B. Beasley and Norman J. Pullman**, Linear operators that strongly preserve the index of imprimitivity

890 **Jerry Donato**, The Boltzmann equation with lie and cartan

891 **Thomas R. Hoffend Jr., Peter Smereka and Roger J. Anderson**, Method for resolving the laser induced local heating of moving magneto-optical recording media